Cancer Letters 459 (2019) 15–29

Contents lists available at ScienceDirect

Cancer Letters

journal homepage: www.elsevier.com/locate/canlet

Original Articles

Oncolytic Ad co-expressing decorin and Wnt decoy receptor overcomes chemoresistance of desmoplastic tumor through degradation of ECM and inhibition of EMT

Yan Li[a], JinWoo Hong[b], Bo-Kyeong Jung[b], Eonju Oh[b], Chae-Ok Yun[b,c,*]

[a] Biomarker Branch, National Cancer Center, 323 Ilsan-ro, Ilsandong-gu, Goyang-si, Gyeonggi-do, 10408, Republic of Korea
[b] Department of Bioengineering, College of Engineering, Hanyang University, 222 Wangsimni-ro, Seongdong-gu, Seoul, 04763, Republic of Korea
[c] Institute of Nano Science and Technology (INST), Hanyang University, 222 Wangsimni-ro, Seongdong-gu, Seoul, 04763, Republic of Korea

ARTICLE INFO

Keywords:
Decorin
sLRP6E1E2
Oncolytic adenovirus
Pancreatic cancer
Metastasis
Extracellular matrix
Chemosensitivity

ABSTRACT

Pancreatic cancer is a highly lethal disease. Excessive accumulation of tumor extracellular matrix (ECM) and epithelial-to-mesenchymal transition (EMT) phenotype are two main contributors to drug resistance in desmoplastic pancreatic tumors. To overcome desmoplasia and chemoresistance of pancreatic cancer, we utilized an oncolytic adenovirus (Ad) co-expressing decorin and soluble Wnt decoy receptor (HEmT-DCN/sLRP6). An orthotopic pancreatic xenograft tumor model was established in athymic nude mice using Mia PaCa-2 cells, and the antimetastatic and antitumor efficacy of systemically administered HEmT-DCN/sLRP6 was evaluated. Immunohistochemical analysis of tumor tissues was performed to assess ECM degradation, induction of apoptosis, viral dispersion, and inhibition of the Wnt/β-catenin signaling pathway. HEmT-DCN/sLRP6 effectively degraded tumor ECM and inhibited EMT, leading to enhanced viral distribution, induction of apoptosis, and attenuation of tumor cell proliferation in tumor tissue. HEmT-DCN/sLRP6 prevented metastasis of pancreatic cancer. Importantly, HEmT-DCN/sLRP6 sensitized pancreatic tumor to gemcitabine treatment. Furthermore, HEmT-DCN/sLRP6 augmented drug penetration and dispersion within pancreatic tumor xenografts and patient-derived tumor spheroids. Collectively, these results illustrate that HEmT-DCN/sLRP6 can enhance the dispersion of both oncolytic Ad and a chemotherapeutic agent in chemoresistant and desmoplastic pancreatic tumor, effectively overcoming the preexisting limitations of standard treatments.

1. Introduction

Pancreatic cancer, the fourth leading cause of cancer mortality, remains one of the most difficult cancers to treat [1–3]. Currently available treatment options for pancreatic cancer, such as chemotherapy, radiotherapy, and surgery, have shown limited efficacy, with a 5-year survival rate of only 6% [4]. Gemcitabine, a chemotherapeutic agent that causes termination of DNA synthesis and induces apoptosis, is currently the standard treatment for patients with advanced and metastatic pancreatic cancer, but the 1-year survival rate on gemcitabine is very low at 17–23% due to the inherent drug resistance of pancreatic cancer [5–12].

Pancreatic cancer generally demonstrates rapid and anomalous growth of extracellular matrix (ECM) and a highly activated Wnt pathway [13,14]. Previous studies have shown that the ECM plays a prominent role in creating a barrier against the penetration and distribution of drugs within the tumor tissues, resulting in low therapeutic efficacy and poor disease control [15–17]. Furthermore, both increased ECM density and activation of Wnt signaling pathway can promote epithelial-to-mesenchymal transition (EMT), which further contributes to the drug-resistant phenotype of cancer [17,18]. Activation of the Wnt signaling pathway also promotes progression and metastasis of pancreatic cancer, making it an attractive therapeutic target for treatment [19].

To address these obstacles to pancreatic cancer treatment, we utilized an oncolytic adenovirus (Ad) that co-expresses decorin (DCN) and soluble Wnt decoy receptor (sLRP6E1E2). DCN, a small leucine-rich proteoglycan ubiquitously present in ECM, promotes ECM remodeling through binding to collagen fibrils, which delays the lateral assembly of individual triple helical collagen molecules. In addition, DCN blocks the activity of transforming growth factor-β (TGF-β), further suppressing the production of various ECM components [20–22]. sLRP6E1E2, which consists of the E1 and E2 regions of lipoprotein receptor related protein 6 (LRP6), inhibits canonical Wnt signaling and induces

* Corresponding author. Department of Bioengineering, College of Engineering, Hanyang University, 222 Wangsimni-ro, Seongdong-gu, Seoul, Republic of Korea.
E-mail address: chaeok@hanyang.ac.kr (C.-O. Yun).

https://doi.org/10.1016/j.canlet.2019.05.033
Received 16 September 2018; Received in revised form 24 May 2019; Accepted 24 May 2019

apoptosis via mitogen-activated protein kinase and phosphatidylinositol 3-kinase pathways [23]. Moreover, sLRP6E1E2 has been shown to inhibit EMT, a major contributor to metastasis and chemoresistance, by upregulation of epithelial markers and downregulation of mesenchymal markers [23].

Given the clinical potential of DCN in ECM remodeling and of sLRP6E1E2 as an antimetastatic agent, oncolytic Ad co-expressing DCN and sLRP6E1E2 (HEmT-DCN/sLRP6) could induce a potent therapeutic effect when administered to pancreatic tumors. We demonstrate for the first time that HEmT-DCN/sLRP6 efficiently degrades tumor ECM and inhibits metastasis by expression of DCN and sLRP6E1E2. Importantly, HEmT-DCN/sLRP6-mediated downregulation of EMT markers and degradation of ECM lead to chemosensitization of pancreatic cancer to gemcitabine treatment, resulting in a potent and synergistic antitumor effect.

2. Materials and methods

2.1. Cell lines and cell culture

HEK293 cells (human embryonic kidney cell line expressing the Ad E1 region), pancreatic cancer cell lines (MIA PaCa-2, PANC-1, and AsPC-1), human lung cancer cells (A549), and normal human fibroblast cell lines (HDF and BJ) were purchased from the American Type Culture Collection (ATCC, Manassas, VA). Human normal pancreatic cells (NPC) were purchased from Applied Biological Materials Inc. (ABM, Richmond, Canada). All cell lines with the exception of AsPC-1, NPC, BJ, and HMEC were cultured in Dulbecco's modified Eagle's medium (DMEM; GIBCO BRL, Grand Island, NY) supplemented with 10% fetal bovine serum (FBS; GIBCO BRL) and penicillin-streptomycin (100 IU/mL; GIBCO BRL). AsPC-1, NPC, and BJ cells were maintained in RPMI-1640 (GIBCO BRL), prigrow I medium (ABM), and modified Eagle's medium (MEM; GIBCO BRL), respectively. All cell lines were maintained at 37 °C in a humidified atmosphere at 5% CO_2.

2.2. Animal studies

Six to eight-week-old male athymic nude mice were purchased from Charles River Korea (Seongnam, South Korea) and maintained in a laminar air flow cabinet under specific pathogen-free environment. All facilities were approved by AAALAC (Association for Assessment and Accreditation of Laboratory Animal Care). All of the animal experiments were conducted according to the institutional guidelines established for the Hanyang University Institutional Animal Care and Use Committee.

2.3. Construction and preparation of oncolytic Ad co-expressing decorin and sLRP6E1E2

The preparation of an oncolytic Ad co-expressing DCN and FLAG-tagged sLRP6E1E2 was described in a previous study [23,24]. Replication-incompetent Ad (dE1-k35) and oncolytic Ad (ONYX-015) were used as control Ads and were propagated in 293 cells. HEmT-DCN/sLRP6 was propagated in A549 cells. The vector construct of HEmT-DCN/sLRP6 is provided as Supplementary Fig. S1. All Ads were purified by CsCl (Sigma, St Louis, MO) gradient centrifugation. The number of viral particles (VP) was calculated from optical density measurements at 260 nm (OD_{260}), where 1 absorbency unit (OD_{260} = 1) is equivalent to 1.1×10^{12} VP/mL. Purified viruses were stored at −80 °C until use. The VP-to-infectious unit (PFU) ratio was assumed to be 100:1 for multiplicity of infection (MOI) calculation of *in vitro* experiments as described previously [25].

2.4. Western blot analysis

MIA PaCa-2 pancreatic cancer cells cultured in 100-mm plates were infected with HEmT-DCN/sLRP6 at MOI of 2, 5, and 10. At 2 days post-infection, cells and supernatants were harvested, and immunoblotting was performed as described previously [26]. Blocked membranes were incubated with DCN-specific antibody (Ab; R&D Systems, Minneapolis, MN) or FLAG-specific Ab (Sigma) overnight at 4 °C. Bound Abs were detected by a horseradish peroxidase-conjugated rabbit anti-goat secondary Ab (Kirkegaard & Perry Laboratories, Gaithersburg, MD) or a horseradish peroxidase-conjugated horse anti-mouse secondary Ab (Cell Signaling Technology, Beverly, MA) and developed using the enhanced chemiluminescence system (Pierce, Rockford, IL).

2.5. Enzyme-linked immunosorbent assay (ELISA) for secreted decorin

MIA PaCa-2 pancreatic cancer cells cultured in 60-mm plates were infected with HEmT-DCN/sLRP6 at MOI of 2, 5, and 10. At 2 days post-infection, supernatants were collected by centrifugation at 15,000 × *g* for 10 min at 4 °C, and secreted DCN protein was quantified using an ELISA kit (Abcam, Cambridge, UK).

2.6. Cytopathic effect assay

To evaluate the cytopathic effect (CPE) of oncolytic Ad infection, cells (pancreatic cancer cells: AsPC-1, PANC-1, and MIA PaCa-2; normal cells: NPC, BJ, and HDF) were plated on 24-well plates and grown until approximately 60%–70% confluent. Cells were treated with dE1-k35, ONYX-015, or HEmT-DCN/sLRP6 at 0–50 MOI. Replication-incompetent Ad (dE1-k35) was used as a negative control. At 3 days post-infection, plates were stained with 0.5% crystal violet in 50% methanol for 1 h, washed with water, and dried.

2.7. MTT assay

The cytotoxicity of gemcitabine was determined by measuring conversion of the tetrazolium salt 3-(4,5-dimethylthiazolyl-2)-2,5diphenyltetrazolium bromide (MTT, Sigma) to formazan. Pancreatic cancer cells (MIA PaCa-2, PANC-1, and AsPC-1) were detached by trypsinization, seeded at 5×10^4 cells per well in a 24-well plate overnight, and treated with various concentrations (0–100 μg/mL) of gemcitabine in DMEM with 10% FBS. After 3 days of incubation at 37 °C, 200 μL of MTT in phosphate-buffered saline (PBS; 2 mg/mL) was added to each well. After incubation at 37 °C for 4 h, the supernatant was discarded, and the precipitate was dissolved in 1 mL of dimethyl sulfoxide (DMSO). Plates were read on a microplate reader at 540 nm. For combination therapy with oncolytic Ad and gemcitabine, pancreatic cancer cells were seeded as described above and then infected with HEmT-DCN/sLRP6 at MOI of 0.5 and 2. At 24 h post-infection, cells were treated with gemcitabine (0.2 μg/mL). At 48 h after treatment with gemcitabine, the MTT assay was carried out. All assays were performed in triplicate.

2.8. Orthotopic model of human pancreatic cancer

MIA PaCa-2 cells (5×10^6 cells/50 μL), which stably express firefly luciferase, were injected beneath the capsule of the pancreas of athymic nude mice (Charles River Korea, Seoul, Korea), and the abdominal wall and skin were closed. At 2 weeks post-implantation (week 0), mice were divided into three groups to receive intraperitoneal treatment with PBS, ONYX-015, or HEmT-DCN/sLRP6 (n = 6, each group) on weeks 0, 1, and 2. Optical imaging was performed on weeks 0, 1, 2, 3, 4, and 5 with IVIS SPECTRUM (Xenogen, Alameda, CA). Imaged signals were quantitatively analyzed with IGOR-PRO Living Image software (Xenogen). At 12 weeks after the first treatment, tumors and several organs were collected, imaged, and weighed.

To evaluate the combination therapy of oncolytic Ad and gemcitabine, tumor models were prepared under the same conditions as above. At 2 weeks post-implantation (week 0), mice were divided into four

groups (PBS, gemcitabine, HEmT-DCN/sLRP6, or HEmT-DCN/sLRP6 plus gemcitabine; n = 4, each group) and treated intraperitoneally with Ad (2×10^{10} VP/mouse on days 0, 2, and 4) and/or gemcitabine twice a week for 3 weeks. Optical imaging was carried out on weeks 0, 1, 2, and 3 with IVIS SPECTRUM, and imaged signals were quantitatively analyzed with IGOR-PRO Living Image software. At 3 weeks after the first treatment, tumors were collected and sectioned.

2.9. Histology and immunohistochemistry

Tumor tissue or liver was harvested at 3 weeks after the first treatment, fixed in 4% paraformaldehyde, and embedded in paraffin wax for histologic examination and immunohistochemical staining. Representative sections were stained with hematoxylin and eosin (H & E), Masson's trichrome, or picrosirius red and examined by light microscopy (Carl Zeiss Inc., Thornwood, NY). The tumor sections were also incubated at 4 °C overnight with rabbit anti-Ad E1A (Santa Cruz Biotechnology, Santa Cruz, CA), anti-mouse proliferating cell nuclear antigen (PCNA; DAKO, Glostrup, Denmark), mouse anti-collagen type I (Abcam), mouse anti-collagen type III (Sigma), mouse anti-elastin (Sigma), or mouse anti-fibronectin (Santa Cruz Biotechnology) primary Abs and then incubated at room temperature for 20 min with the Dako Envision™ Kit (DAKO) as secondary Ab. Diaminobenzidine/hydrogen peroxidase (DAKO) was used as the chromogen substrate. All slides were counterstained with Mayer's hematoxylin.

2.10. Terminal deoxynucleotidyl transferase dUTP nick end labeling assay

The 5-μm formalin-fixed paraffin-embedded tissue sections were deparaffinized and rehydrated according to standard protocols [27]. Apoptosis was detected with the terminal deoxynucleotidyl transferase dUTP nick end labeling (TUNEL) assay (DeadEndTM Fluorometric TUNEL System; Promega, Madison, WI). Briefly, tissue sections were permeabilized with proteinase K (20 mg/mL) for 10 min at room temperature. Sections were then incubated with terminal deoxynucleotidyl transferase (TdT) and fluorescein-12-dUTP in TdT buffer at room temperature for 1 h and washed with TdT buffer. Finally, nuclei were counterstained with methyl green. The samples were analyzed by light microscopy.

2.11. Immunofluorescence staining

For immunofluorescence staining of Wnt, β-catenin, vimentin, matrix metalloproteinase 2 (MMP-2), or MMP-9, tumor sections were treated with mouse anti-Wnt3a (Santa Cruz Biotechnology), rabbit anti-β-catenin (Cell Signaling Technology), mouse anti-vimentin (Abcam), rabbit anti-MMP-2 (Abcam), or rabbit anti-MMP-9 (Abcam) primary Abs and incubated overnight at 4 °C. Next, the tumor sections were treated with Alexa Fluor 488 (green)-conjugated goat anti-mouse IgG (Invitrogen, Carlsbad, CA) or Alexa Fluor 488 (green)-conjugated goat anti-rabbit IgG (Invitrogen) Ab at room temperature for 1 h. For counterstaining, the samples were incubated with 4,6-diamidino-2-phenylindole (Sigma). The slides were mounted with Vectashield mounting medium (Vector Laboratories, Burlingame, CA) and imaged under a fluorescence microscope (Carl Zeiss Inc.)

2.12. Assessment of drug penetration in pancreatic cancer xenograft and cancer patient-derived tumor spheroids

MIA PaCa-2 cells (5×10^6 cells/50 μL) were injected subcutaneously into the right abdomen of 6- to 7-week-old male athymic nude mice. When the tumor volume reached approximately 100 mm^3 (day 0), mice were sorted into two groups with similar mean tumor volumes and received intratumoral treatment (PBS or HEmT-DCN/sLRP6) (n = 3, each group) on days 0, 2, and 4. Doxorubicin (DOX) was administered intratumorally on days 3 and 5. At 6 h after the last treatment with DOX, tumors were frozen in optimal cutting temperature (OCT) compound (Sakura Finetec, Torrance, CA) and cut into 9-μm sections. The slides were mounted with Vectashield mounting medium, and cells were viewed under a DeltaVision system (Applied Precision, Issaquah, WA). Fluorescence intensity of DOX measured in Gray value was plotted against distance away from the center of tumor spheroid using ImageJ software (version 1.50b; U.S. National Institutes of Health, Bethesda, MD).

Tumor samples were obtained from patients with active-stage ovarian cancer, and patient-derived tumor spheroids were prepared as previously described [22]. The plates containing tumor spheroids were treated twice with PBS or oncolytic Ad (5×10^{10} VP of HEmT-DCN/sLRP6) on days 1 and 3. On day 4, each tumor spheroid was treated with DOX (50 μM) and incubated at 37 °C. At 6 h after treatment with DOX, tumor spheroids were frozen, and the slides were prepared as described above then observed under a fluorescence microscope.

2.13. Assessment of liver toxicity

To analyze potential *in vivo* toxicity, serum was harvested 3 weeks after the first treatment, and the levels of aspartate aminotransferase (AST) and alanine transaminase (ALT) were measured.

2.14. Statistical analysis

Statistical comparisons were performed using Stat View software (Abacus Concepts, Inc., Berkeley, CA) and Mann-Whitney test (non-parametric rank sum test). The data are expressed as mean ± standard deviation (SD). P values less than 0.05 were considered statistically significant ($^*P < 0.05$, $^{**}P < 0.01$, or $^{***}P < 0.001$).

To calculate the combination index (CI), Chou-Talalay method for drug combination analysis was performed with CompuSyn software (available for free download from www.combosyn.com) where CI < 1, = 1, and > 1 indicates synergism, additive effect, and antagonism, respectively [28].

3. Results

3.1. Oncolytic Ad-mediated decorin and sLRP6E1E2 expression

To assess the level of DCN expression mediated by HEmT-DCN/sLRP6, MIA PaCa-2 cells were treated with HEmT-DCN/sLRP6 at various MOIs. Two days after infection, the expression level of DCN in culture supernatants or cell lysates was assessed by ELISA or western blot analysis, respectively. As shown in Fig. 1A, dose-dependent DCN expression was observed in both culture supernatants and lysates of pancreatic cancer cells treated with HEmT-DCN/sLRP6. Next, we analyzed whether the cells effectively expressed FLAG-tagged sLRP6E1E2 following infection with HEmT-DCN/sLRP6. Cells treated with HEmT-DCN/sLRP6 showed a dose-dependent increase in the expression level of sLRP6E1E2 in both cell lysates and supernatants (Fig. 1B). Together, these results demonstrate that both DCN and sLRP6E1E2 can be efficiently expressed and secreted from cancer cells following infection with HEmT-DCN/sLRP6.

3.2. Cytopathic effect of oncolytic Ad co-expressing decorin and sLRP6E1E2

To compare the cancer cell-specific killing effect of HEmT-DCN/sLRP6 and commercially available oncolytic Ad (ONYX-015; a strain similar to oncolytic Ad H101 that is currently marketed as Oncorine) [29–31], various pancreatic cancer and normal cells were treated with each virus at 0 to 50 MOI, with replication-incompetent dE1-k35 included as a negative control (Fig. 1C). HEmT-DCN/sLRP6 induced a significantly enhanced cancer cell killing effect compared with ONYX-015 in various pancreatic cancer cells (MIA PaCa-2, PANC-1, and AsPC-

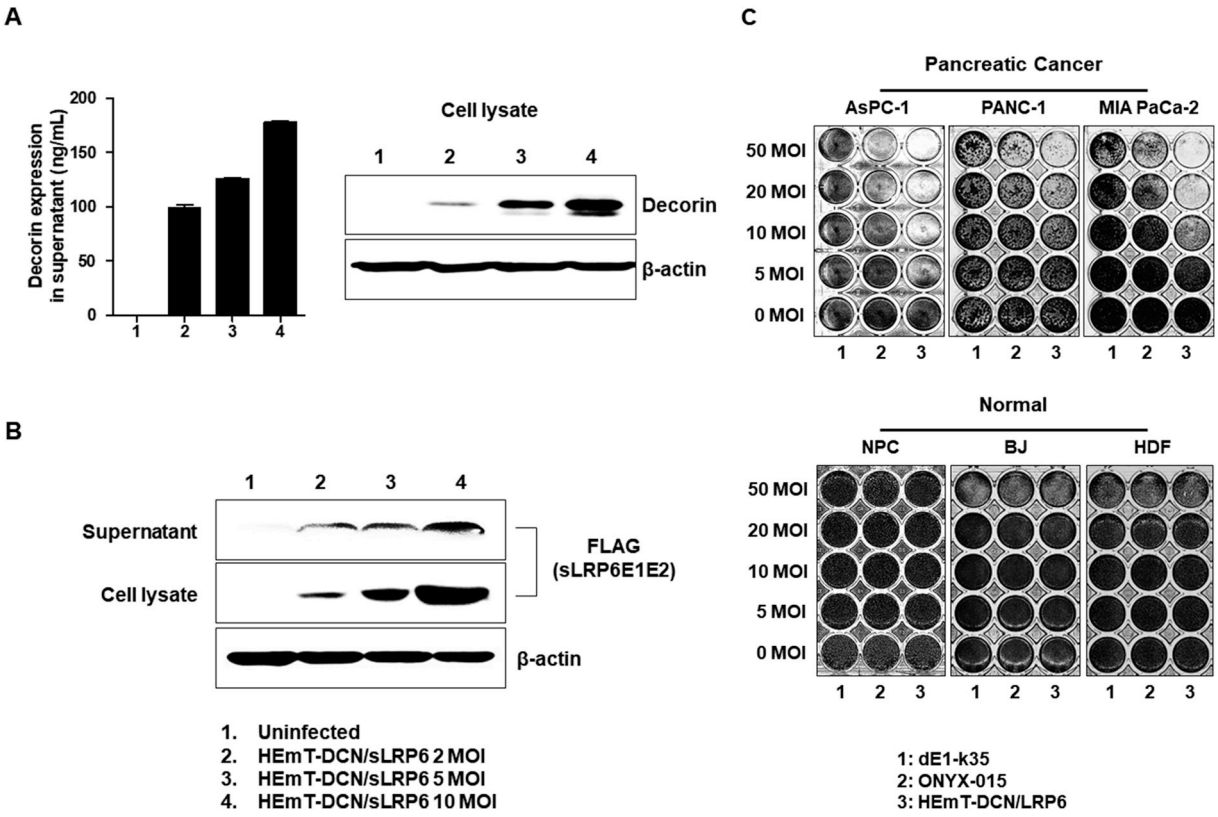

Fig. 1. HEmT-DCN/sLRP6-induced DCN and sLRP6E1E2 expression. MIA PaCa-2 pancreatic cancer cells were infected for 48 h with HEmT-DCN/sLRP6 at a multiplicity of infection (MOI) of 2, 5, or 10. (A) Expression of DCN was analyzed in culture supernatant or cell lysates by ELISA or immunoblot analysis, respectively. (B) Expression level of FLAG epitope-tagged sLRP6E1E2 was analyzed in culture supernatant and cell lysate by immunoblot analysis. ELISA was performed in triplicate, and data are presented as mean ± SD. The data of immunoblot analysis are representative of three independent experiments. (C) Cytopathic effect of Ads in cancer and normal cells. Monolayers of cancer and normal cells were treated with dE1-k35 (lane 1), ONYX-015 (lane 2), or HEmT-DCN/sLRP6 (lane 3) at MOI ranging from 0 to 50. Replication-incompetent Ad (dE1-k35) served as a negative control.

1), suggesting that HEmT-DCN/sLRP6 elicits more potent anticancer efficacy than the clinically approved ONYX-015 for the treatment of pancreatic cancer. Importantly, HEmT-DCN/sLRP6 elicited minimal cytopathic effects in normal cells (NPC, BJ, and HDF) in a similar manner as ONYX-015. Together, these results demonstrate that HEmT-DCN/sLRP6 induces potent anticancer activity against pancreatic cancer with good specificity.

3.3. Potent therapeutic efficacy of oncolytic Ad co-expressing decorin and sLRP6E1E2 in an orthotopic pancreatic model

Orthotopic models of pancreatic cancer emulate the key aspects of aggressive human pancreatic cancer, and the kinetics of disease progression in such models are highly reproducible, making them well-suited for preclinical testing of novel therapeutics [24,32,33]. To evaluate the therapeutic efficacy of HEmT-DCN/sLRP6, nude mice with MIA PaCa-2 orthotopic pancreatic tumors were intraperitoneally injected 3 times with 5×10^{10} VP of ONYX-015 or HEmT-DCN/sLRP6 on weeks 0, 1, and 2, with PBS as a negative control. As shown in Fig. 2A, tumors of PBS- or ONYX-015-treated mice continued to grow substantially for 5 weeks following the initial treatment, whereas mice treated with HEmT-DCN/sLRP6 exhibited a marked reduction in tumor burden. At 5 weeks post-treatment, the increase in total flux of tumor from mice treated with PBS- or ONYX-015 was 15.1- or 13.8-fold higher than the initial measurement, whereas the HEmT-DCN/sLRP6-treated group showed a 0.2-fold lower total flux during the same time interval (Fig. 2B). The potent antitumor efficacy of HEmT-DCN/sLRP6 led to significant tumor growth inhibition with respect to PBS- and ONYX-015-treated mice, showing 94.0% and 93.0% inhibition, respectively (***$P < 0.001$). At 12 weeks post-treatment, the tumor weight measurement exhibited similar results to photon measurements, with the HEmT-DCN/sLRP6-treated tumors weighing the least (Fig. 2C; ***$P < 0.001$).

3.4. Potent inhibition of tumor metastasis by treatment with oncolytic Ad co-expressing decorin and sLRP6E1E2

To assess the antimetastatic effect of HEmT-DCN/sLRP6, a spontaneous metastasis model was established by implanting MIA PaCa-2 pancreatic cancer cells into the pancreas, which induced metastasis to the peritoneum. As shown in Fig. 3A and B, PBS- or ONYX-015-treated groups had multiple metastatic colonies in the mesentery, whereas HEmT-DCN/sLRP6-treated mice exhibited no observable metastasis (Fig. 3A and B; ***$P < 0.001$, versus PBS or ONYX-015). Importantly, HEmT-DCN/sLRP6 inhibited metastases to other organs in addition to mesentery, suggesting that HEmT-DCN/sLRP6-mediated expression of sLRP6E1E2 can efficiently prevent metastasis of aggressive pancreatic cancer (Fig. 3C and D).

The native tropism of Ad toward coxsackievirus and adenovirus receptor (CAR)-mediated internalization into host cells results in non-specific sequestration in the liver, causing hepatotoxicity. Furthermore, the presence of extensive metastatic lesions in the liver has been associated with hepatotoxicity and attenuated liver function [34]. Therefore, Ad-mediated hepatotoxicity was assessed in liver tissue by H & E and E1A staining and measurement of AST/ALT levels following treatment with PBS, ONYX-015, or HEmT-DCN/sLRP6. The liver tissue of mice treated with ONYX-015 was noticeably stiffer and reduced in size (Fig. 3C). In marked contrast, the HEmT-DCN/sLRP6-treated group

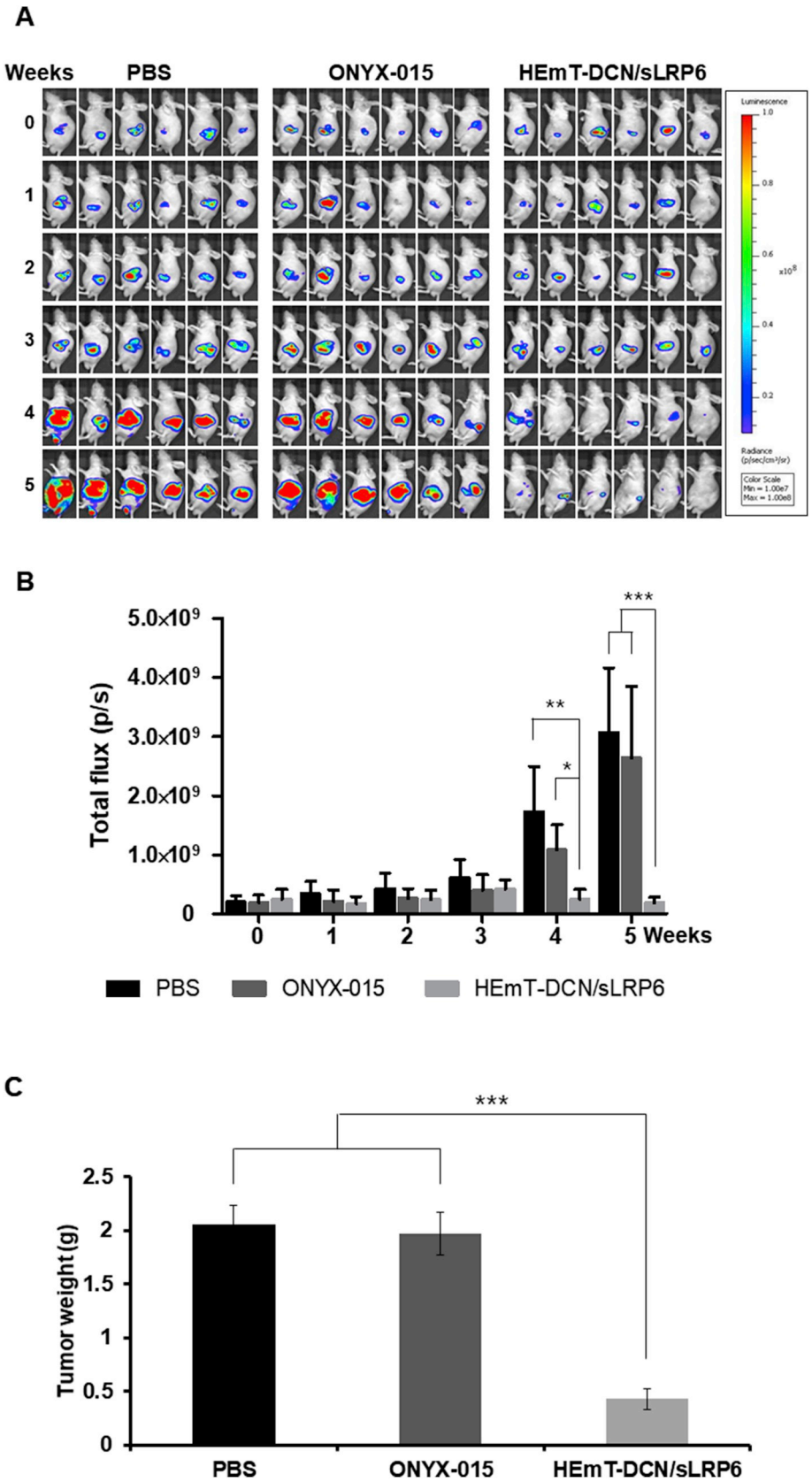

Fig. 2. Antitumor efficacy of oncolytic Ads in an orthotopic pancreatic tumor xenograft model. Nude mice bearing firefly luciferase-expressing MIA PaCa-2 orthotopic pancreatic tumors were intraperitoneally treated a total of three times (week 0, 1, and 2) with PBS, ONYX-015, or HEmT-DCN/sLRP6. (A) MIA PaCa-2 tumors were monitored by optical imaging of luciferase expression every week. (B) Average optical signal intensity displayed as photons acquired per second (p/s). (C) Tumor weight measurement at 12 weeks after the initial treatment. Data represent mean ± SD. $^{*}P < 0.05$, $^{**}P < 0.01$, or $^{***}P < 0.001$.

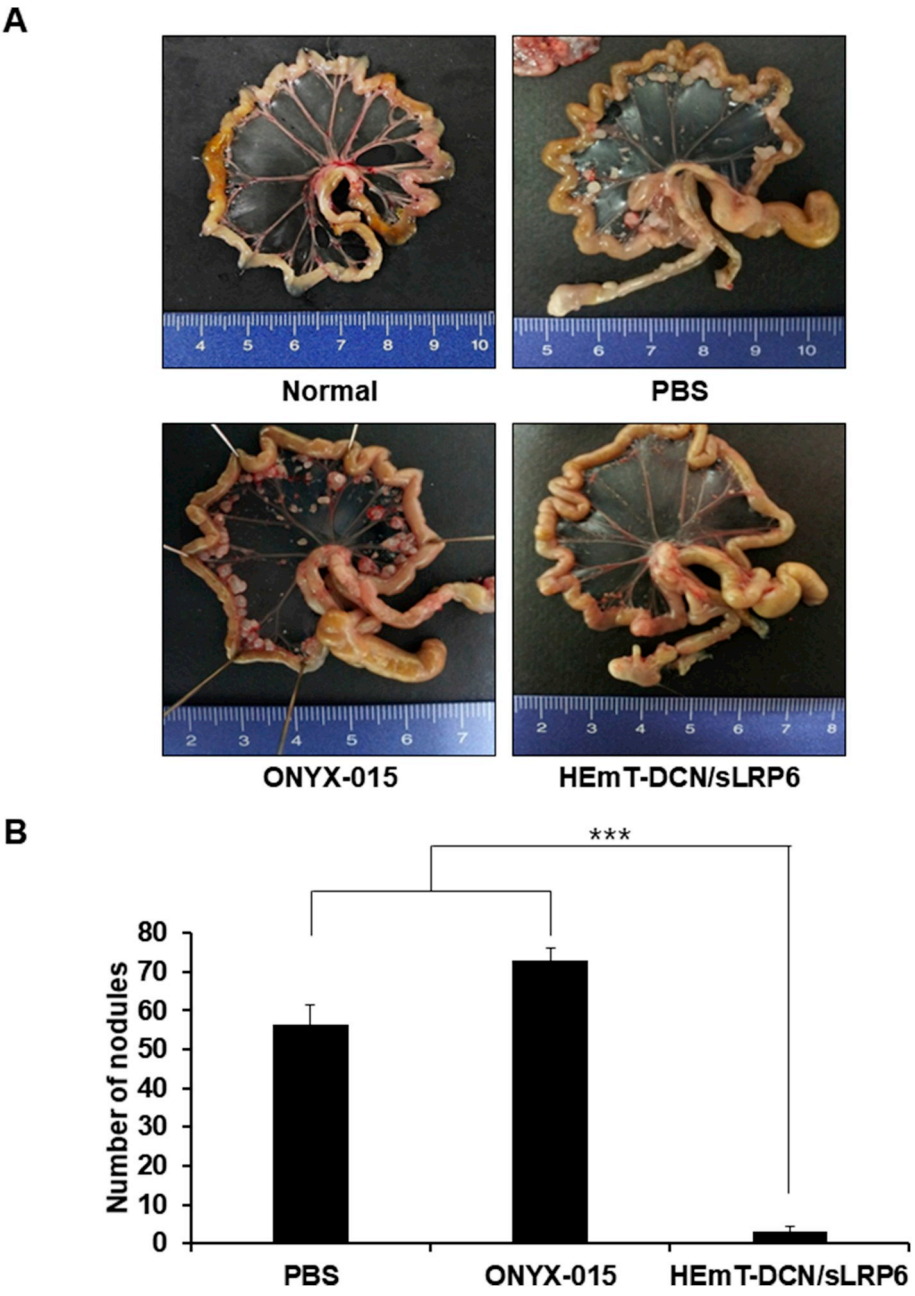

Fig. 3. Assessment of metastasis inhibition and hepatotoxicity induced by oncolytic Ads. Nude mice bearing MIA PaCa-2 orthotopic pancreatic tumors were intraperitoneally treated a total of 3 times (week 0, 1, and 2) with PBS, ONYX-015, or HEmT-DCN/sLRP6. Mice were sacrificed on either the 3rd or 12th week after the first administration to assess hepatotoxicity or metastasis inhibition, respectively. (A, B) The metastatic nodules in the mesentery were photographed and counted. (C, D) Bioluminescence was measured and quantified in the pancreas and other organs within the abdominal cavity. (E) Histopathological assessment of liver harvested at 3 weeks after the first treatment. Representative sections were stained with H & E and E1A. (F) Serum AST and ALT levels were measured 3 weeks after the first treatment. Data represent mean ± SD. $^{*}P < 0.05$, $^{**}P < 0.01$, or $^{***}P < 0.001$.

showed no observable conformational changes in liver tissue, which exhibited a similar size and morphology to that of the PBS-treated group. In support of these observations, H & E staining of liver tissues demonstrated that ONYX-015 treatment causes severe hepatotoxicity, as evidenced by nuclear pyknosis and abundant infiltration of inflammatory cells (Fig. 3E). In marked contrast, HEmT-DCN/sLRP6-treated mice exhibited normal liver histology. Moreover, Ad E1A staining revealed that there was no observable Ad accumulation in the liver tissues following systemic administration of HEmT-DCN/sLRP6, whereas the liver tissues of ONYX-015-treated mice were highly E1A-positive (Fig. 3E). These results suggest that systemically administered ONYX-015 is nonspecifically sequestered to hepatic tissues, likely due to CAR-dependent internalization while HEmT-DCN/sLRP6 uptake is restricted by its Ad serotype 5/35 chimeric fiber, which has been shown to reduce hepatic accumulation of Ad [35]. Analysis of serum ALT and AST levels following systemic administration of each treatment showed similar results to those of histological analysis (Fig. 3F). Specifically, both PBS- and ONYX-015-treated mice showed significantly elevated levels of AST compared to those of normal mice without tumor ($^{**}P < 0.01$). Importantly, HEmT-DCN/sLRP6-treated mice exhibited AST and ALT levels similar to those of normal mice, indicating that HEmT-DCN/sLRP6 did not induce significant hepatotoxicity.

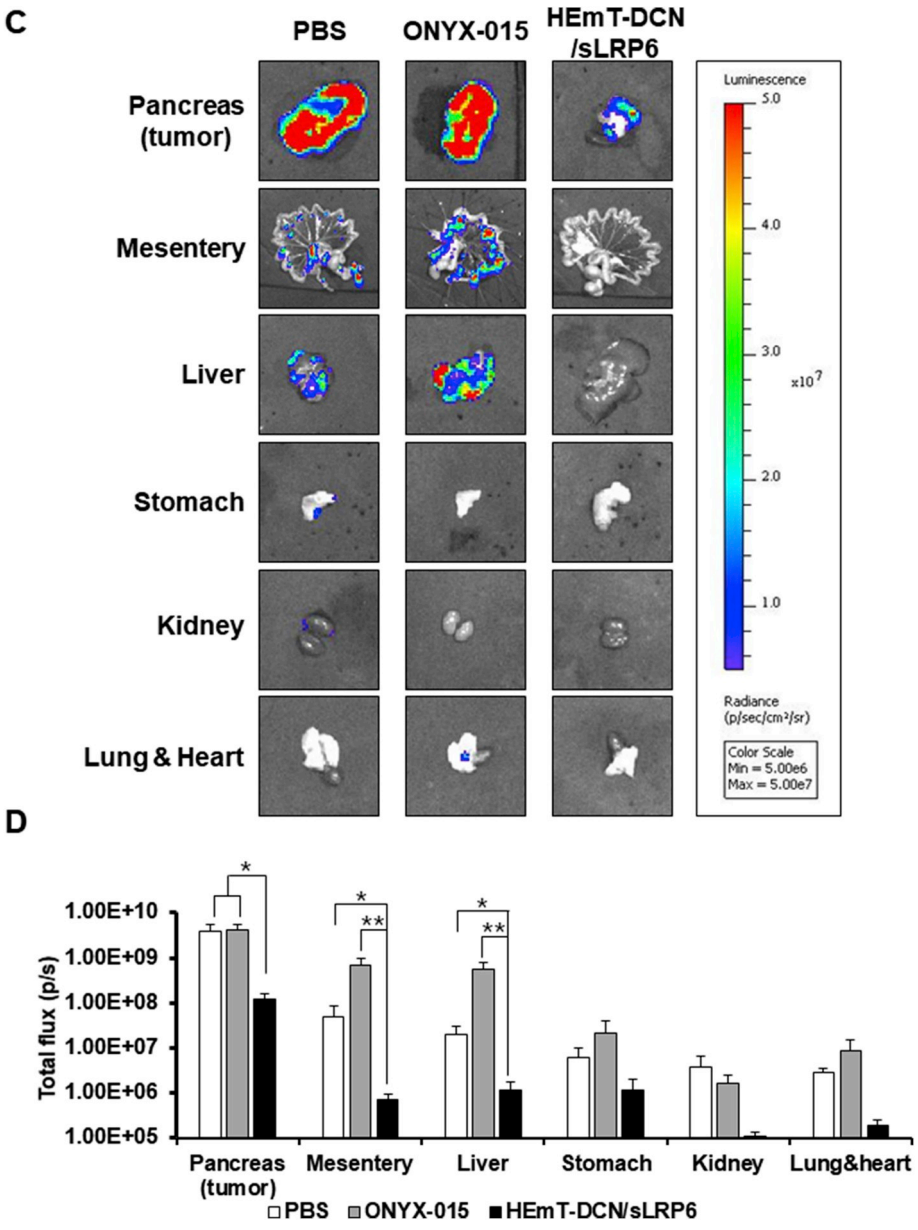

Fig. 3. (*continued*)

3.5. Histological, TUNEL, and immunohistochemical characterization

To further investigate the therapeutic effect and replication of oncolytic Ad, tumor tissues were harvested 3 weeks after the administration of initial treatment (PBS, ONYX-015, or HEmT-DCN/sLRP6) and assessed by histological and immunohistochemical analyses. H & E staining revealed markedly reduced numbers of viable tumor cells and extensive necrotic regions in HEmT-DCN/sLRP6-treated tumors compared with PBS- or ONYX-015-treated tumors (Fig. 4A). Masson's trichrome and picrosirius red staining revealed extensive accumulation of collagen and ECM in tumor tissues treated with PBS or ONYX-015, demonstrating the highly desmoplastic nature of pancreatic cancer (Fig. 4A). In marked contrast, HEmT-DCN/sLRP6-treated tumors were free from aberrant tumor ECM, suggesting that DCN expression by HEmT-DCN/sLRP6 can degrade aberrant ECM and restrict the desmoplastic reaction of pancreatic cancer. As shown in Fig. 4B, HEmT-DCN/sLRP6-treated tumors exhibited significantly attenuated accumulation of major ECM components such as collagen type I, collagen type III, elastin, and fibronectin compared with tumors treated with PBS or ONYX-015. These findings indicate that oncolytic Ad-mediated expression of DCN effectively degrades overexpressed ECM components in desmoplastic pancreatic tumors.

Importantly, HEmT-DCN/sLRP6-treated tumors, which showed complete degradation of aberrant tumor ECM, exhibited markedly higher accumulation of the virus compared with tumors treated with ONYX-015, indicating a strong positive correlation between ECM degradation and antitumor efficacy of oncolytic Ad. TUNEL staining revealed that most regions of HEmT-DCN/sLRP6-treated tumor tissue were apoptotic, whereas apoptotic lesions were not detectable or detected at a markedly lower frequency in PBS- or ONYX-015-treated tumor tissues, respectively. In line with these results, HEmT-DCN/sLRP6-treated tumors showed a markedly lower quantity of proliferating tumor cells than those treated with ONYX-015, reaffirming the superior antitumor efficacy of HEmT-DCN/sLRP6 (Fig. 4C).

A constitutively activated Wnt signaling pathway can induce EMT signaling and MMP expression [23,36,37], which contribute to the progression and aggressiveness of cancer. Given these findings, the effect of each treatment on the expression level of EMT-related factors within tumor tissue was assessed by immunofluorescence analysis. As shown in Fig. 4D, high expression levels of mesenchymal markers (Wnt,

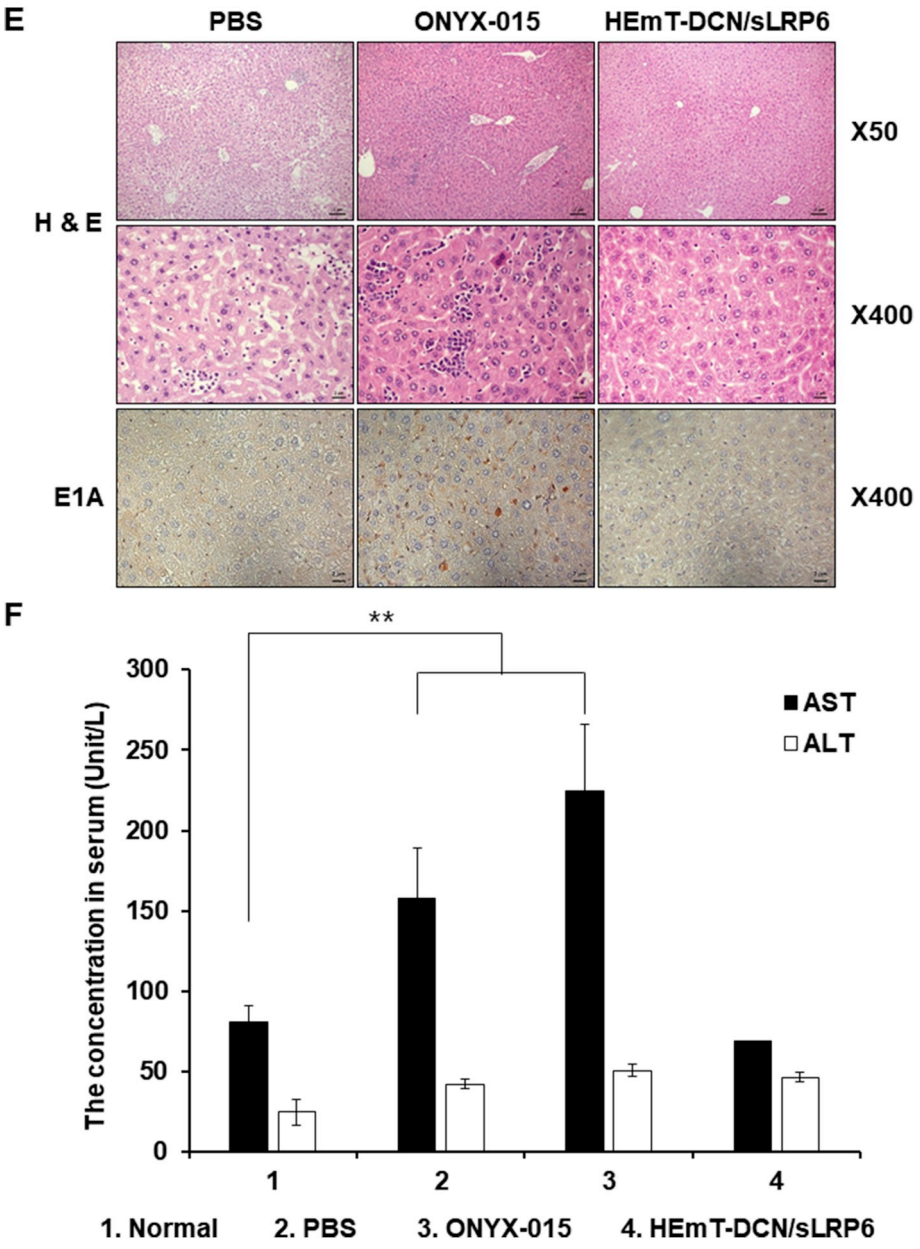

Fig. 3. (*continued*)

β-catenin, and vimentin) were observed in PBS- or ONYX-015-treated tumors, indicating that the Wnt/β-catenin signaling pathway was highly active in these tumor tissues. In marked contrast, HEmT-DCN/sLRP6-treated tumors showed markedly lower quantities of Wnt, β-catenin, and vimentin, demonstrating that expression of soluble Wnt decoy receptor can effectively inhibit Wnt/β-catenin signaling pathway in pancreatic cancer. Concordant with these results, HEmT-DCN/sLRP6-treated tumors also exhibited markedly lower expression levels of MMP-2 and MMP-9 than tumors treated with PBS or ONYX-015 through effective inhibition of the Wnt signaling cascade. Together, these results demonstrate that HEmT-DCN/sLRP6 can effectively degrade tumor ECM and prevent EMT, leading to potent antitumor efficacy.

3.6. HEmT-DCN/sLRP6-mediated restoration of chemosensitivity in pancreatic cancer cells

To investigate the chemosensitizing effect of HEmT-DCN/sLRP6 on chemoresistant pancreatic cancer cells, the cancer cell killing effects of gemcitabine as a single therapeutic agent or in combination with HEmT-DCN/sLRP6 were analyzed. Several chemoresistant pancreatic cancer cells [38] were treated with gemcitabine at concentrations ranging from 0.05 to 100 μg/mL. As shown in Fig. 5A, treatment of AsPC-1, PANC-1, and MIA PaCa-2 cells with gemcitabine resulted in a dose-dependent cancer cell death up to 5 or 20 μg/mL. Importantly, the therapeutic efficacy of gemcitabine remained consistently low, with more than 70% of pancreatic cancer cells still viable even at a high dose of 100 μg/mL, indicating that these cells are highly chemoresistant. In marked contrast, a low dose of gemcitabine (0.2 μg/mL) in combination with HEmT-DCN/sLRP6 led to a significantly higher cell killing effect than treatment with either gemcitabine or oncolytic Ad alone (Fig. 5B; $^{***}P < 0.001$ in AsPC-1 and PANC-1 cells and $^{*}P < 0.5$ or $^{***}P < 0.001$ in MIA PaCa-2 cells). Specifically, gemcitabine killed 3.2% of AsPC-1 cells when administered alone, whereas combination treatment with oncolytic Ad (0.5 MOI or 2 MOI) resulted in 26.3% and 75.0% cell killing, respectively, demonstrating that combination treatment can elicit a synergistic anticancer effect (CI = 0.002 and 0.000 at 0.5 and 2 MOI, respectively). A similar cell killing effect by

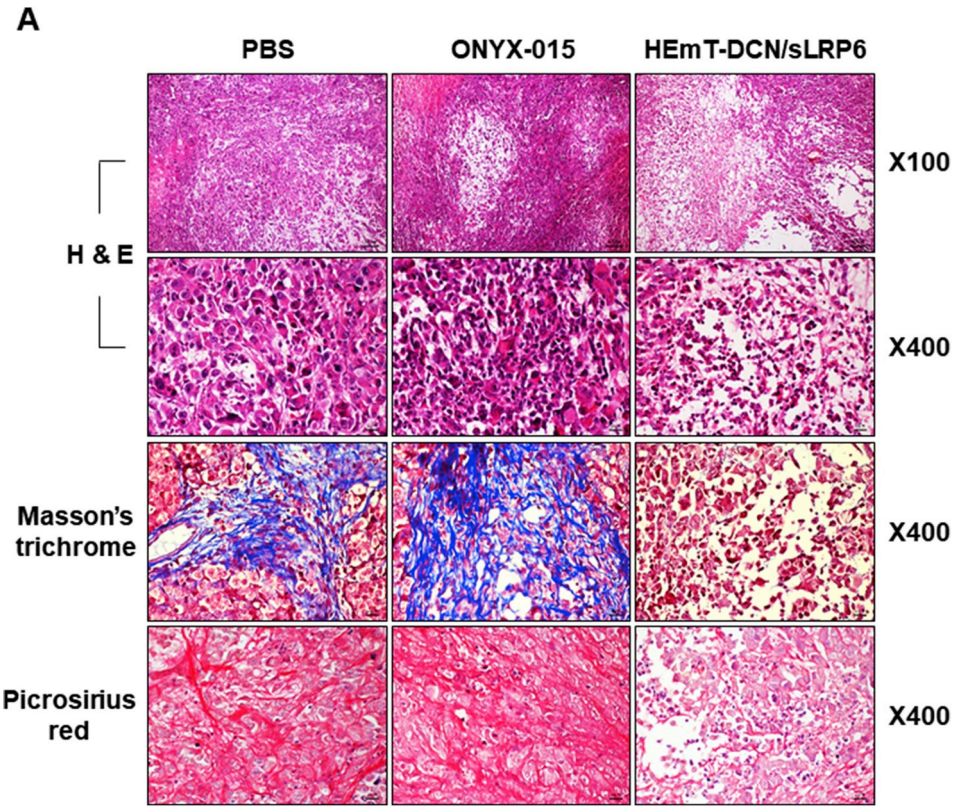

Fig. 4. Histological and immunohistochemical analysis of orthotopic pancreatic tumor tissues. Tumors were harvested 3 weeks after the initial treatment with PBS, ONYX-015, or HEmT-DCN/sLRP6. (A) H & E, Masson's trichrome, and picrosirius red staining of tumor tissue. Original magnification: ×100 and ×400. (B) Immunohistochemical analysis of major ECM components (collagen type I and III, elastin, and fibronectin). Original magnification: ×400. (C) Ad E1A, TUNEL, and PCNA staining of pancreatic tumor tissue. Original magnification: ×400. (D) Immunofluorescence staining of Wnt, β-catenin, vimentin, MMP-2, and MMP-9 in tumor tissue. Original magnification: ×200.

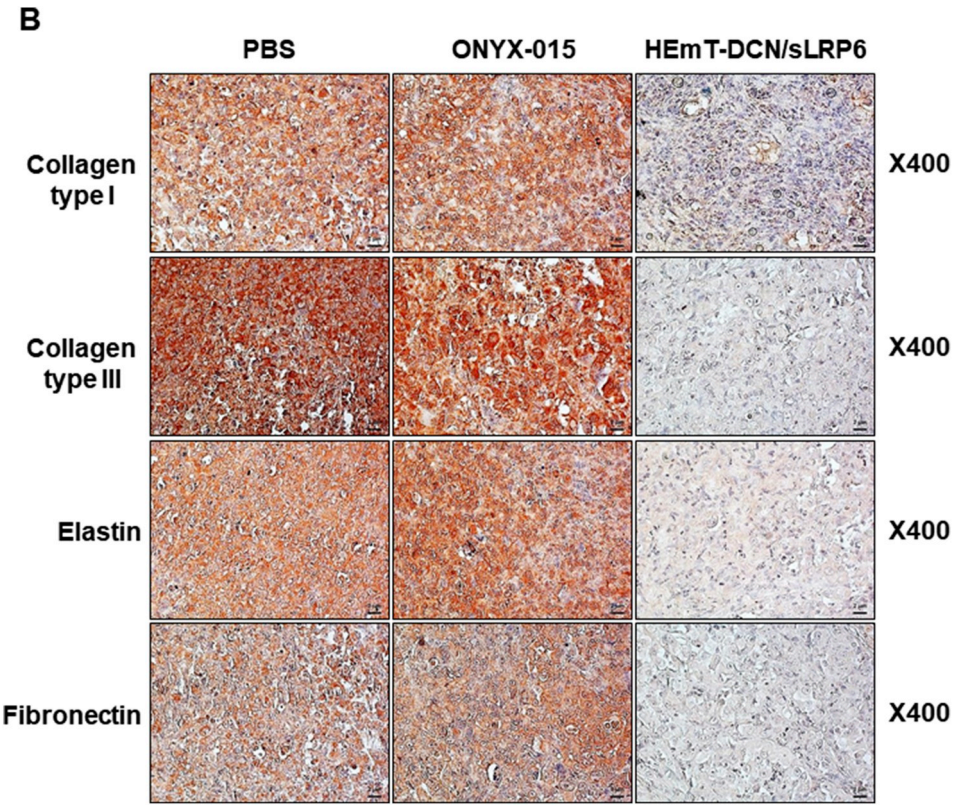

Fig. 4. (*continued*)

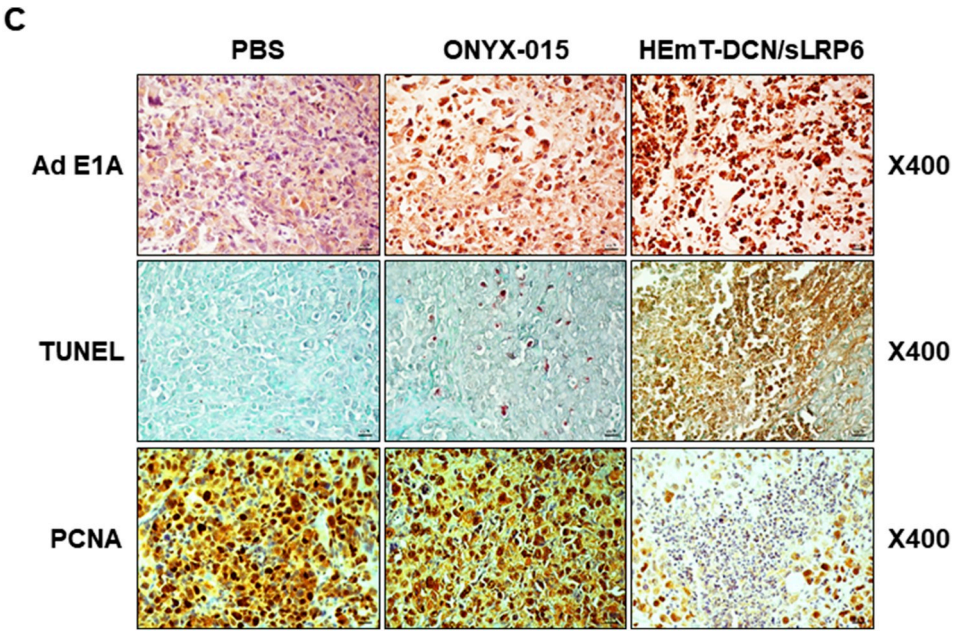

Fig. 4. (*continued*)

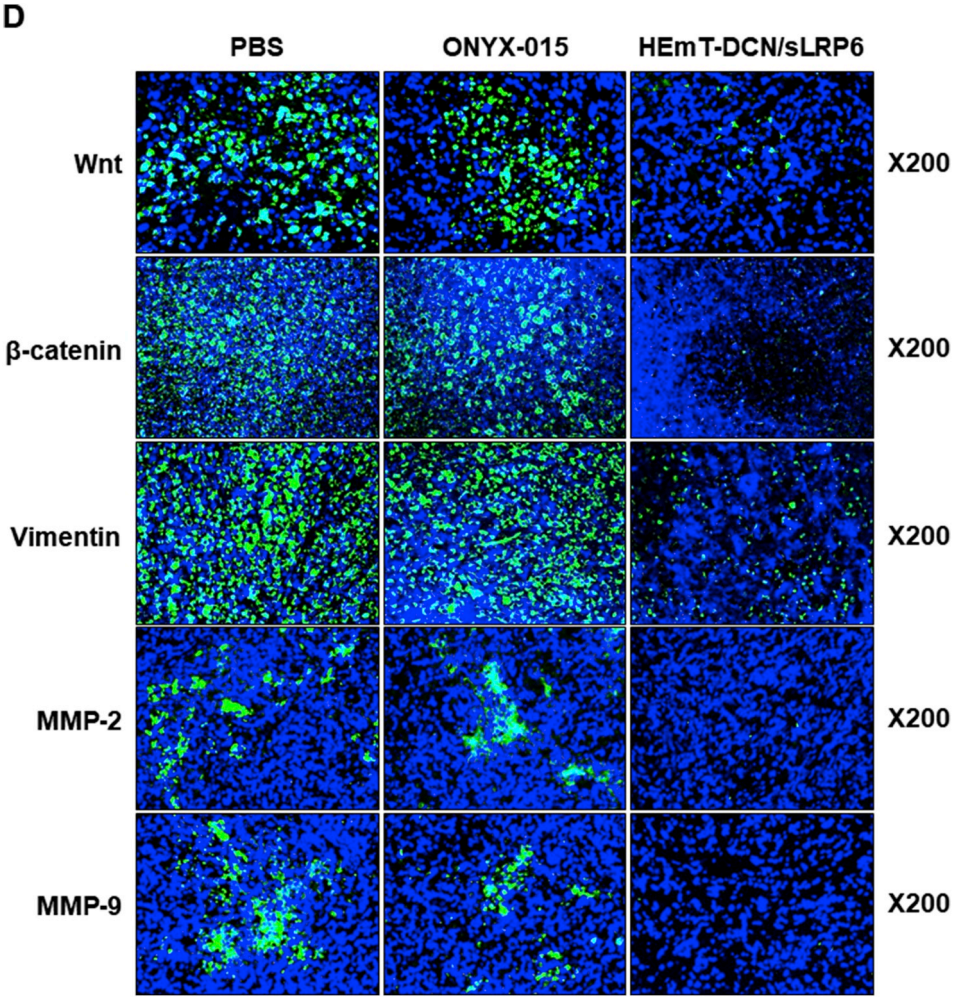

Fig. 4. (*continued*)

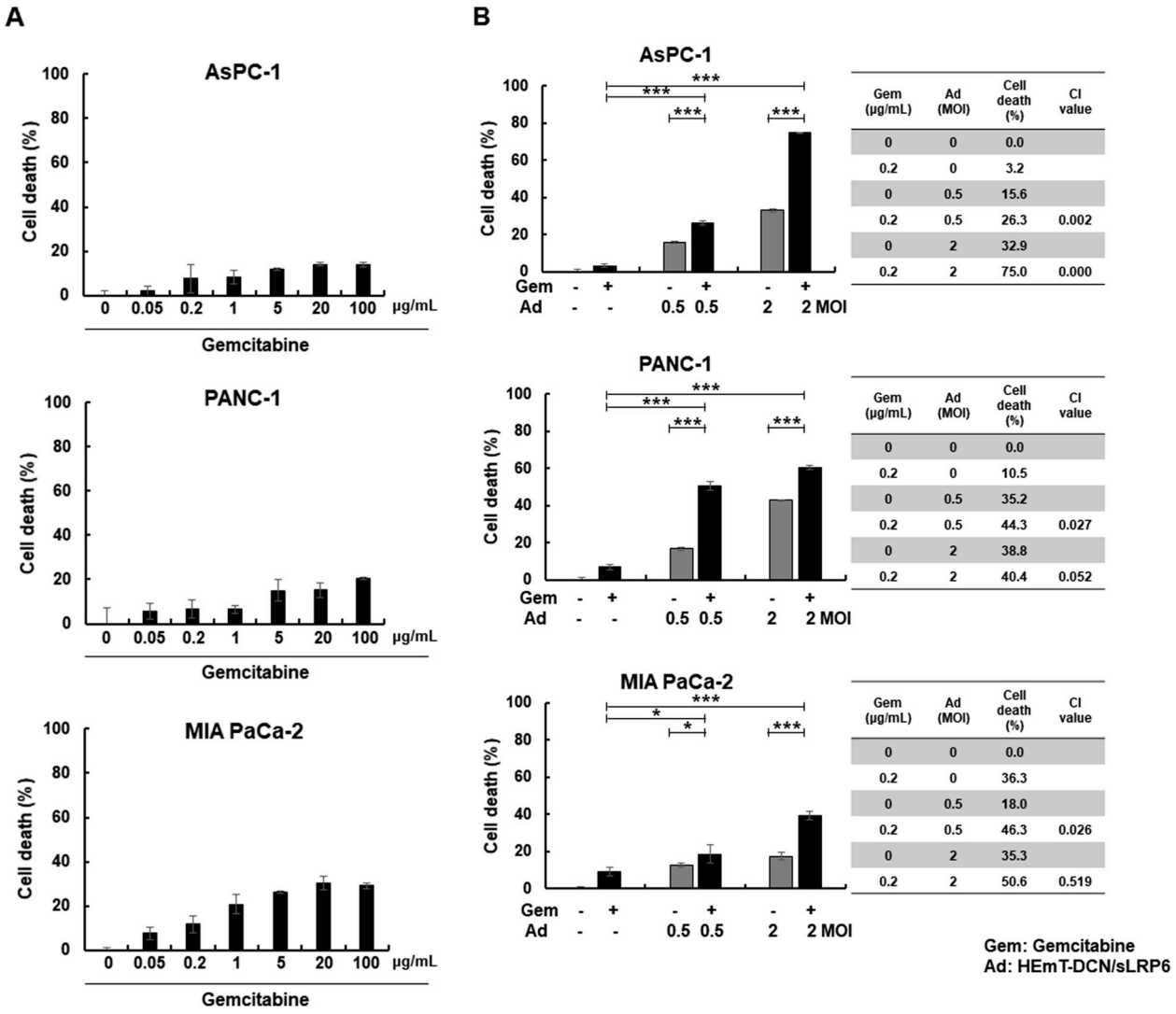

Fig. 5. Cancer cell killing efficacy of gemcitabine monotherapy and combination therapy with oncolytic Ad. (A) Cancer cell killing efficacy of gemcitabine monotherapy in chemoresistant pancreatic cancer cells (AsPC-1, PANC-1, and MIA PaCa-2). Cells were exposed to 0.05, 0.2, 1, 5, 20, or 100 μg/mL gemcitabine for 3 days, and the cytotoxicity of gemcitabine was determined by MTT assay. The results are expressed as percentage of remaining viable cells compared with the untreated group. Data shown are representative of three independent experiments with triplicate samples per group. Bars represent mean ± SD. (B) Cancer cell killing efficacy of HEmT-DCN/sLRP6 and gemcitabine combination therapy. Cells were treated with PBS, gemcitabine, HEmT-DCN/sLRP6, or HEmT-DCN/sLRP6 plus gemcitabine. Gemcitabine was administered at a final concentration of 0.2 μg/mL, and cells were infected with HEmT-DCN/sLRP6 at an MOI of 0.5 or 2. Data shown are representative of three independent experiments, which were performed with triplicate samples. Bars represent mean ± SD. (*$P < 0.05$, ***$P < 0.001$). (C-E) Antitumor efficacy of HEmT-DCN/sLRP6 and gemcitabine combination therapy in orthotopic pancreatic xenograft tumor model. Two weeks after the implantation of MiaPaCa-2 cells (week 0), mice were randomly allocated for treatment with PBS, gemcitabine, HEmT-DCN/sLRP6, or HEmT-DCN/sLRP6 plus gemcitabine. Mice received 3 intraperitoneal injections of HEmT-DCN/sLRP6 on days 0, 2, and 4, whereas gemcitabine was administered intraperitoneally twice a week for 3 weeks. (C,D) Firefly luciferase expression was monitored every week after treatment. Data represent mean ± SD for total flux measurement (*$P < 0.05$). (E) H & E, PCNA, TUNEL, and Ad E1A staining of tumor tissues. Original magnification: ×400.

combination therapy was observed in MIA PaCa-2 and PANC-1 cells. Taken together, these results indicate that HEmT-DCN/sLRP6 can sensitize highly chemoresistant pancreatic cancer toward gemcitabine and elicit a synergistic cancer cell killing effect in combination with gemcitabine.

3.7. Potent antitumor effect against orthotopic pancreatic tumor xenograft by combination of oncolytic Ad and gemcitabine

To assess the antitumor effect of HEmT-DCN/sLRP6 in combination with gemcitabine, human orthotopic pancreatic xenograft tumors were treated with PBS, gemcitabine, HEmT-DCN/sLRP6, or HEmT-DCN/sLRP6 plus gemcitabine (Fig. 5C). For the combination treatment, mice received an intraperitoneal injection of HEmT-DCN/sLRP6 on days 0, 2, and 4 at a 2.5-fold lower dose than used in the previous monotherapy experiment (2×10^{10} VP/injection versus 5×10^{10} VP/injection from Fig. 2), and gemcitabine was administered intraperitoneally twice a week for 3 weeks (days 3, 7, 11, 14, 18, and 21). At 3 weeks post-treatment, the average increase in total flux in the PBS, gemcitabine, HEmT-DCN/sLRP6, and combination groups was 21.3-, 9.6-, 4.9- and 1.9- fold higher, respectively, than the initial measurement. Importantly, combination treatment inhibited tumor growth by 77.9% or 62.3% compared with gemcitabine or HEmT-DCN/sLRP6 monotherapy, respectively (Fig. 5D; *$P < 0.05$ versus PBS group). These results demonstrate that the combination of HEmT-DCN/sLRP6 and gemcitabine can be an effective strategy to induce a potent antitumor effect against highly chemoresistant pancreatic tumor.

For further assessment of the antitumor effect mediated by each

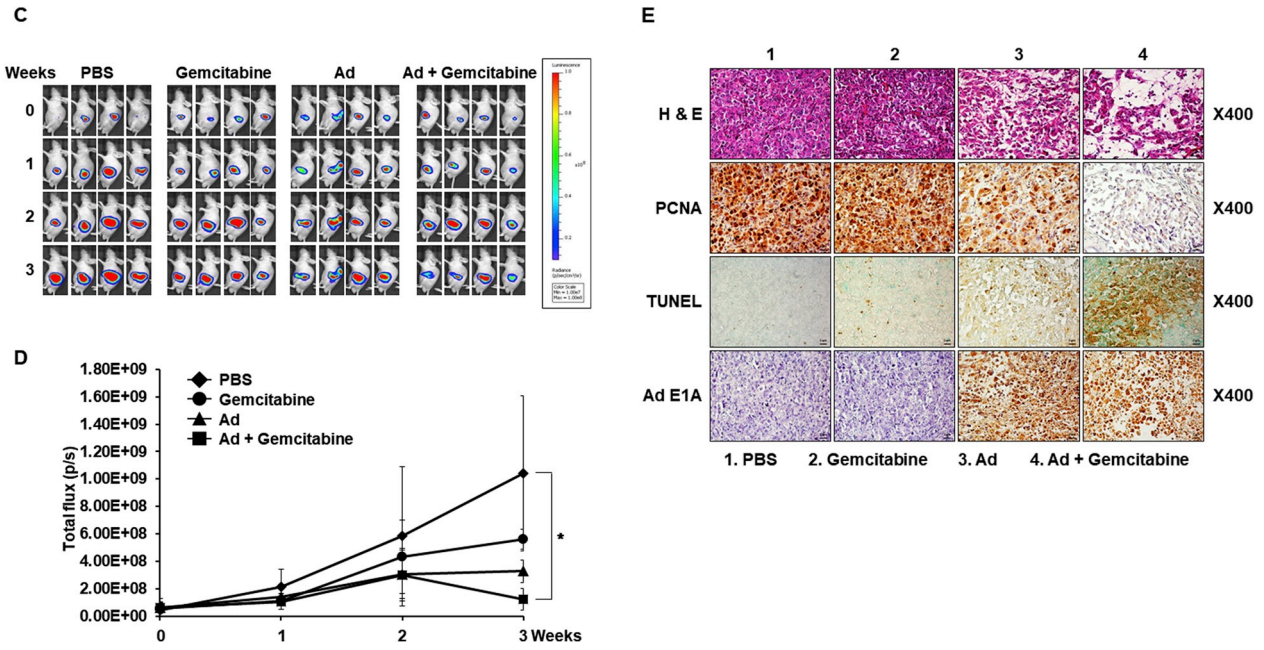

Fig. 5. (*continued*)

treatment group, tumor tissues harvested in the 3rd week after initial treatment were analyzed by histology and immunohistochemistry. As shown in Fig. 5E, H & E staining revealed large areas of proliferating tumor cells in either PBS- or gemcitabine-treated tissues, whereas moderate or extensive necrosis was observed in HEmT-DCN/sLRP6 or HEmT-DCN/sLRP6 plus gemcitabine groups, respectively. PCNA and TUNEL staining revealed that tumor tissues treated with HEmT-DCN/sLRP6 plus gemcitabine showed a markedly lower quantity of proliferating tumor cells and higher incidence rate of apoptosis compared with any other treatment group, further supporting the notion that combination treatment induces the most potent antitumor effect. Furthermore, both HEmT-DCN/sLRP6 monotherapy and HEmT-DCN/sLRP6 plus gemcitabine treatment resulted in efficient dispersion of oncolytic Ad within tumor tissue, indicating that gemcitabine did not impede the spread of oncolytic Ad.

3.8. HEmT-DCN/sLRP6-mediated enhancement of drug penetration and dispersion in pancreatic tumor xenograft and patient-derived tumor spheroids

To investigate the effect of HEmT-DCN/sLRP6 on dispersion of chemotherapeutic agent in pancreatic cancer xenograft tumors, subcutaneously established pancreatic tumors were intratumorally injected 3 times with HEmT-DCN/sLRP6 (5×10^{10} VP) on days 0, 2, and 4, and DOX was administered intratumorally on days 3 and 5 for the combination treatment group. As shown in Fig. 6A, DOX monotherapy resulted in poor drug dispersion within the central region of tumor xenografts. In marked contrast, HEmT-DCN/sLRP6-treated tumor tissues showed greatly enhanced dispersion of DOX in both peripheral and central tumor regions compared with the DOX monotherapy group.

Next, the effect of HEmT-DCN/sLRP6 on drug penetration in tumors was analyzed using patient-derived tumor spheroids. As shown in Fig. 6B, tumor spheroids treated with a combination of HEmT-DCN/sLRP6 and DOX showed markedly enhanced penetration of DOX compared with those treated with DOX monotherapy. Together, these results demonstrate that HEmT-DCN/sLRP6 can enhance drug penetration and dispersion in highly desmoplastic tumors.

4. Discussion

Orthotopic tumor models provide a unique opportunity to study a human malignancy in a context that is as close as possible to the clinical condition [33]. Therefore, the therapeutic efficacy of HEmT-DCN/sLRP6 was evaluated using an orthotopic pancreatic tumor model in which the tumors closely emulate the pathophysiological progression and desmoplasia of pancreatic cancer in the clinic [32]. Because of the deep intra-abdominal location of orthotopic pancreatic cancer, 2 different methods (photon flux measurement by bioluminescent imaging and endpoint tumor weight measurement) were utilized to track and assess tumor growth. Both methods yielded similar results, with HEmT-DCN/sLRP6 showing superior tumor growth inhibition compared with commercialized ONYX-015 (Fig. 2), owing to more effective replication of HEmT-DCN/sLRP6 in tumor tissues following systemic administration (Supplementary Fig. S4).

The viral replication and antitumor effect by ONYX-015 was likely restricted and attenuated compared to HEmT-DCN/sLRP6 due to the deletion of Ad E1B 55 kDa gene. Although E1B 55 kDa gene deletion was the pioneering strategy to endow Ad with cancer specificity and numerous adaptations of said strategy being reported by various groups [39–42], the approach is no longer actively being pursued due to well-known attenuation to viral replication [43–45]. Thus, only a minute fraction of oncolytic Ads in on-going clinical trials harbor E1B 55 kDa gene deletion [46]. Due to these reasons, ONYX-015 as control will likely elicit suboptimal therapeutic effect in comparison to more recently developed oncolytic Ads.

The potent antitumor efficacy of HEmT-DCN/sLRP6 was mediated by two distinctive mechanisms: (1) DCN-mediated effective degradation of tumor ECM enhances the distribution of oncolytic Ad within solid tumor; and (2) the expression of sLRP6E1E2 and subsequent inhibition of Wnt/β-catenin signaling pathway can inhibit proliferation of tumor cells and induce apoptotic tumor cell death [23,24].

Additionally, HEmT-DCN/sLRP6 could be safely administered via systemic injection as no Ad-associated hepatotoxicity was observed, whereas commercialized ONYX-015 induced hepatotoxicity and elicited insufficient antitumor efficacy against pancreatic cancer (Fig. 3D and E). This is probably because HEmT-DCN/sLRP6 utilizes Ad serotype 5/35 chimeric fiber, which has been reported to attenuate hepatic sequestration of Ad compared with wild-type Ad serotype 5 fiber [35].

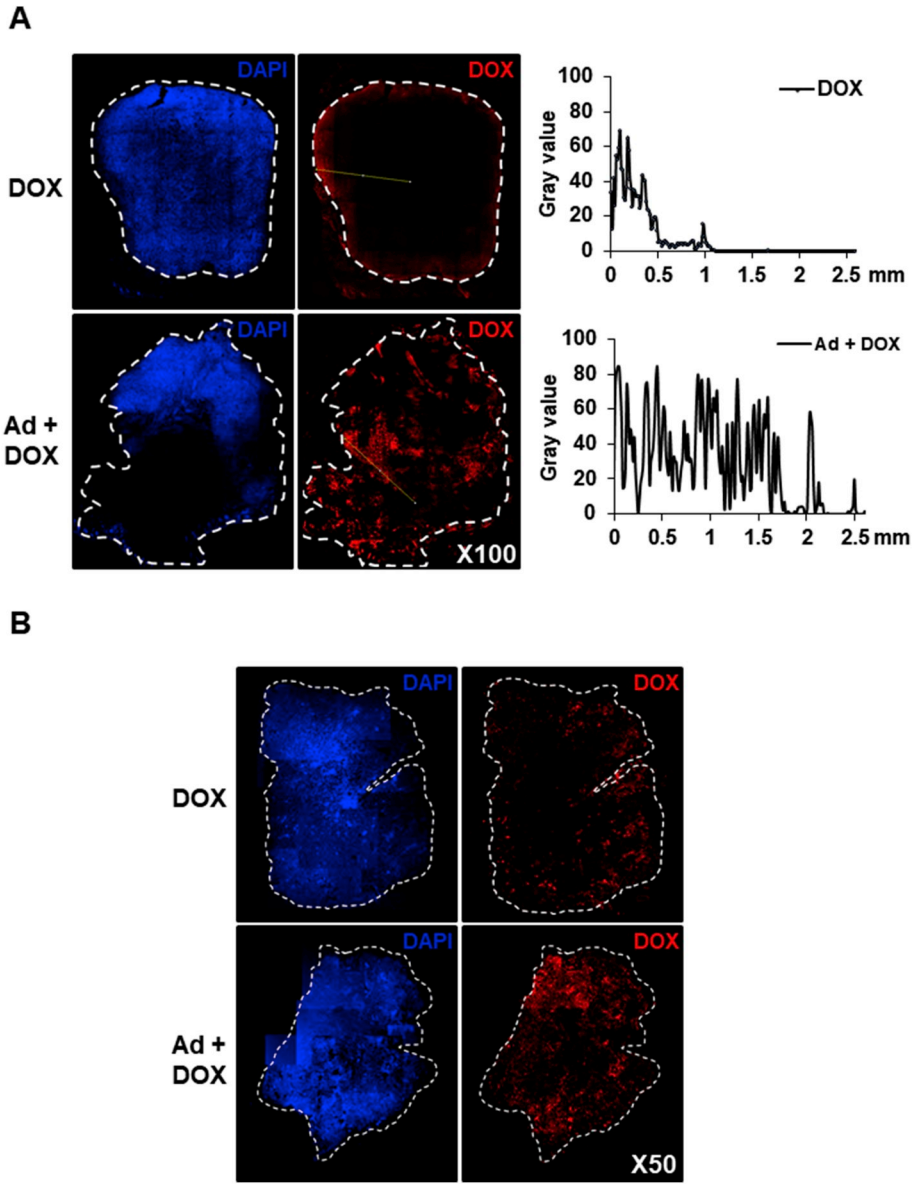

Fig. 6. Assessment of drug penetration and dispersion in pancreatic cancer xenografts and cancer patient-derived tumor spheroids. (A) MIA PaCa-2 cells were injected subcutaneously into the right abdomen of athymic nude mice. When the average tumor volume reached approximately 100 mm^3 (day 0), the mice were randomly allocated for treatment with PBS or HEmT-DCN/sLRP6 by intratumoral injection on day 0, 2, and 4 (n = 3 per group). Doxorubicin (DOX) was administered intratumorally at 7.5 mg/kg on days 3 and 5. At 6 h after the last administration of DOX, the tumors were harvested and viewed under a DeltaVision system. Original magnification: ×50. Fluorescence intensity of DOX measured in Gray value was plotted against distance away from center of the tumor spheroid (white square) using ImageJ software. (B) Evaluation of drug penetration into patient-derived tumor spheroids. Tumor spheroids were generated from patients with active-stage ovarian cancer. The plates containing tumor spheroids were treated twice with PBS or oncolytic Ad (5×10^{10} VP/1 mL of HEmT-DCN/sLRP6) on days 1 and 3. On day 4, each tumor spheroid was treated with DOX (50 μM). At 6 h after treatment with DOX, tumor spheroids were harvested and observed under a fluorescence microscope. Original magnification: ×50.

Furthermore, utilization of serotype 5/35 chimeric fiber for pancreatic cancer is in line with current landscape of oncolytic adenovirus in recent pancreatic cancer clinical trials; as evidenced by LOAd703 in phase I/II clinical trial utilizing serotype 5/35 chimeric fiber [47] (NCT03225989 & NCT02705196) and most clinical trials of oncolytic adenoviruses for other types of cancer in past 5 years utilizing fiber-modified vectors to expand viral tropism and overcome CAR-dependent internalization [48–53]. Consistent with these findings, HEmT-DCN/sLRP6-treated mice showed ALT and AST levels similar to those of healthy mice and we did not observe any Ad E1A in liver tissues via immunohistochemistry, whereas the liver tissues of ONYX-015-treated mice exhibited extensive virion accumulation (Fig. 3E and F). An elevated AST level in PBS-treated is likely caused by extensive liver metastasis (Fig. 3C, D, and F), as others have shown that metastasis to the liver is associated with higher level of serological markers like γ-glutamyltransferase, ALT, and AST [34,54]. Together, these results demonstrated that HEmT-DCN/sLRP6 can be systemically administered in a safe manner to induce potent antitumor efficacy against highly desmoplastic pancreatic cancer.

One of the major obstacles to successful treatment of pancreatic cancer is its propensity for metastasis due to aberrant activation of the Wnt/β-catenin signaling pathway and subsequent EMT [23,55,56]. As shown in Figs. 1 and 3, HEmT-DCN/sLRP6 treatment led to efficient expression and secretion of soluble Wnt decoy receptor (sLRP6E1E2) and effective inhibition of metastasis, suggesting that inactivation of the Wnt signaling pathway by sLRP6E1E2 could prevent metastasis. In support of these claims, HEmT-DCN/sLRP6-treated tumors showed markedly low levels of EMT markers (Wnt, β-catenin, and vimentin) and MMP-2/9, indicating that oncolytic Ad-mediated expression of sLRP6E1E2 could effectively prevent EMT and subsequent metastasis (Fig. 4D). As Wnt signaling has been shown to induce expression of MMP-2/9 through an interaction with Frizzled receptors [37,57], the inhibition of Wnt/β-catenin signaling by soluble decoy receptor likely promoted the suppression of MMP-2/9 expression levels in tumor tissues (Fig. 4D). Of interest, MMP-2 or -9 has recently been shown to cleave and nullify DCN to promote invasion of cancer cells [58,59], suggesting that inhibition of MMP-2/9 by sLRP6 expression may enhance DCN retainment and function in synergistic manner for HEmT-DCN/sLRP6. Additionally, HEmT-DCN/sLRP6 mediated intratumoral expression of DCN, which suppresses the TGF-β level [21,60], and DCN-induced degradation of ECM might further contribute to inhibition of EMT as both the TGF-β signaling pathway and ECM density have been

reported to promote EMT [17,61,62].

The highly drug-resistant phenotype of pancreatic cancer is another critical challenge to successful disease management in the clinic [12,63]. Pancreatic cancer exhibits both biological and physical chemoresistance mechanisms, making it highly refractory to conventional cancer treatment strategies [64–66]. As shown in Fig. 5A, pancreatic cancer cells were highly resistant to gemcitabine *in vitro*, highlighting the biological chemoresistance of pancreatic cancer. This chemoresistant phenotype of pancreatic cancer cells was likely caused by a highly activated Wnt/β-catenin signaling pathway and subsequently upregulated EMT [67]. In support of these inferences, HEmT-DCN/sLRP6, which effectively inhibits the Wnt/β-catenin signaling pathway and EMT (Fig. 4D), sensitized chemoresistant pancreatic cancer cells to gemcitabine treatment and elicited synergistic cancer cell killing when used in combination with gemcitabine (Fig. 5B). Alternatively, the potent chemosensitizing effect of HEmT-DCN/sLRP6 could be attributed to following mechanisms: (1) the expression of the Ad E1A gene has been reported to sensitize cells to apoptotic stimuli [68,69]; or (2) expression of DCN can inhibit activation of the phosphoinositide 3-kinase/AKT signaling pathway [70] that can downregulate apoptosis [71,72].

Desmoplasia, which is characterized by excessive deposition of ECM and concomitant elevation in tumor interstitial fluid pressure, further contributes to the chemoresistant phenotype of pancreatic cancer by functioning as a physical barrier against drug penetration and perfusion [73,74]. Major ECM components, such as several types of collagen and fibronectin, have been reported to increase the resistance of cancer cells to apoptosis and chemotherapeutic agents [12,75,76]. In line with these reports, HEmT-DCN/sLRP6-mediated degradation of tumor ECM and downregulation of its major components (Fig. 4A and B) greatly improved the antitumor efficacy of chemotherapeutic agents against desmoplastic pancreatic tumor (Fig. 5). Furthermore, a strong positive correlation between degradation of major ECM components, dispersion and penetration of chemotherapeutic agent, and induction of apoptosis was observed (Figs. 4B, 5E and 6). Together, these findings demonstrate that HEmT-DCN/sLRP6 can enable both oncolytic Ad and chemotherapeutic drug to overcome the desmoplasia-induced physical drug resistance of pancreatic cancer.

In summary, this is the first demonstration that oncolytic Ad co-expressing DCN and soluble Wnt decoy receptor can effectively degrade ECM components and inhibit Wnt/β-catenin signaling, resulting in potent antitumor efficacy against desmoplastic and rapidly proliferating pancreatic tumor. Importantly, HEmT-DCN/sLRP6 can effectively prevent metastasis of pancreatic cancer and enhances the dispersion of both oncolytic Ad and chemotherapeutic drug in desmoplastic tumor, ultimately enabling both therapeutics to effectively overcome the preexisting limitations of standard treatments.

Competing interests

The authors declare no competing interests.

Acknowledgements

This work was supported by grant from the National Research Foundation of Korea (2016M3A9B5942352; Dr. C-O Yun) and the Research Fund of Hanyang University (HY-2011-G-201100000001880; Dr. C-O Yun).

Appendix A. Supplementary data

Supplementary data to this article can be found online at.https://doi.org/10.1016/j.canlet.2019.05.033.

References

[1] D. Hariharan, A. Saied, H.M. Kocher, Analysis of mortality rates for pancreatic cancer across the world, HPB 10 (2008) 58–62.
[2] J.P. Neoptolemos, D.D. Stocken, H. Friess, C. Bassi, J.A. Dunn, H. Hickey, H. Beger, L. Fernandez-Cruz, C. Dervenis, F. Lacaine, M. Falconi, P. Pederzoli, A. Pap, D. Spooner, D.J. Kerr, M.W. Buchler, C. European Study Group for Pancreatic, A randomized trial of chemoradiotherapy and chemotherapy after resection of pancreatic cancer, N. Engl. J. Med. 350 (2004) 1200–1210.
[3] N.L. Jacobs, F.G. Que, R.C. Miller, S.S. Vege, M.B. Farnell, A. Jatoi, Cumulative morbidity and late mortality in long-term survivors of exocrine pancreas cancer, J. Gastrointest. Cancer 40 (2009) 46–50.
[4] R. Siegel, D. Naishadham, A. Jemal, Cancer statistics, 2013, Ca - Cancer J. Clin. 63 (2013) 11–30.
[5] A.M. Bergman, P.P. Eijk, V.W. Ruiz van Haperen, K. Smid, G. Veerman, I. Hubeek, P. van den Ijssel, B. Ylstra, G.J. Peters, In vivo induction of resistance to gemcitabine results in increased expression of ribonucleotide reductase subunit M1 as the major determinant, Cancer Res. 65 (2005) 9510–9516.
[6] E. Mini, S. Nobili, B. Caciagli, I. Landini, T. Mazzei, Cellular pharmacology of gemcitabine, Ann. Oncol. 17 (Suppl 5) (2006) v7–12.
[7] H.A. Burris 3rd, M.J. Moore, J. Andersen, M.R. Green, M.L. Rothenberg, M.R. Modiano, M.C. Cripps, R.K. Portenoy, A.M. Storniolo, P. Tarassoff, R. Nelson, F.A. Dorr, C.D. Stephens, D.D. Von Hoff, Improvements in survival and clinical benefit with gemcitabine as first-line therapy for patients with advanced pancreas cancer: a randomized trial, J. Clin. Oncol. 15 (1997) 2403–2413.
[8] T. Conroy, F. Desseigne, M. Ychou, O. Bouche, R. Guimbaud, Y. Becouarn, A. Adenis, J.L. Raoul, S. Gourgou-Bourgade, C. de la Fouchardiere, J. Bennouna, J.B. Bachet, F. Khemissa-Akouz, D. Pere-Verge, C. Delbaldo, E. Assenat, B. Chauffert, P. Michel, C. Montoto-Grillot, M. Ducreux, FOLFIRINOX versus gemcitabine for metastatic pancreatic cancer, N. Engl. J. Med. 364 (2011) 1817–1825.
[9] M.J. Moore, D. Goldstein, J. Hamm, A. Figer, J.R. Hecht, S. Gallinger, H.J. Au, P. Murawa, D. Walde, R.A. Wolff, D. Campos, R. Lim, K. Ding, G. Clark, T. Voskoglou-Nomikos, M. Ptasynski, W. Parulekar, G. National Cancer Institute of Canada Clinical Trials, Erlotinib plus gemcitabine compared with gemcitabine alone in patients with advanced pancreatic cancer: a phase III trial of the National Cancer Institute of Canada Clinical Trials Group, J. Clin. Oncol. 25 (2007) 1960–1966.
[10] F. Rivera, S. Lopez-Tarruella, M.E. Vega-Villegas, M. Salcedo, Treatment of advanced pancreatic cancer: from gemcitabine single agent to combinations and targeted therapy, Cancer Treat Rev. 35 (2009) 335–339.
[11] D. Renouf, M. Moore, Evolution of systemic therapy for advanced pancreatic cancer, Expert Rev. Anticancer Ther. 10 (2010) 529–540.
[12] H. Miyamoto, T. Murakami, K. Tsuchida, H. Sugino, H. Miyake, S. Tashiro, Tumor-Stroma Interaction of Human Pancreatic Cancer Acquired Resistance to Anticancer Drugs and Proliferation Regulation Is Dependent on Extracellular MatrixProteins.Pdf > , (2004).
[13] M. Pasca di Magliano, A.V. Biankin, P.W. Heiser, D.A. Cano, P.J. Gutierrez, T. Deramaudt, D. Segara, A.C. Dawson, J.G. Kench, S.M. Henshall, R.L. Sutherland, A. Dlugosz, A.K. Rustgi, M. Hebrok, Common activation of canonical Wnt signaling in pancreatic adenocarcinoma, PLoS One 2 (2007) e1155.
[14] M. Fang, J. Yuan, C. Peng, Y. Li, Collagen as a double-edged sword in tumor progression, Tumour Biol. 35 (2014) 2871–2882.
[15] H. Sauthoff, J. Hu, C. Maca, M. Goldman, S. Heitner, H. Yee, T. Pipiya, W.N. Rom, J.G. Hay, Intratumoral spread of wild-type adenovirus is limited after local injection of human xenograft tumors: virus persists and spreads systemically at late time points, Hum. Gene Ther. 14 (2003) 425–433.
[16] I.K. Choi, R. Strauss, M. Richter, C.O. Yun, A. Lieber, Strategies to increase drug penetration in solid tumors, Front. Oncol. 3 (2013) 193.
[17] S. Kumar, A. Das, S. Sen, Extracellular matrix density promotes EMT by weakening cell-cell adhesions, Mol. Biosyst. 10 (2014) 838–850.
[18] Y. Li, T.G. VandenBoom 2nd, D. Kong, Z. Wang, S. Ali, P.A. Philip, F.H. Sarkar, Up-regulation of miR-200 and let-7 by natural agents leads to the reversal of epithelial-to-mesenchymal transition in gemcitabine-resistant pancreatic cancer cells, Cancer Res. 69 (2009) 6704–6712.
[19] P.A. Beachy, S.S. Karhadkar, D.M. Berman, Tissue repair and stem cell renewal in carcinogenesis, Nature 432 (2004) 324–331.
[20] K.G. Vogel, M. Paulsson, D. Heinegard, Specific inhibition of type I and type II collagen fibrillogenesis by the small proteoglycan of tendon, Biochem. J. 223 (1984) 587–597.
[21] Y. Yamaguchi, D.M. Mann, E. Ruoslahti, Negative regulation of transforming growth factor-beta by the proteoglycan decorin, Nature 346 (1990) 281–284.
[22] I.K. Choi, Y.S. Lee, J.Y. Yoo, A.R. Yoon, H. Kim, D.S. Kim, D.G. Seidler, J.H. Kim, C.O. Yun, Effect of decorin on overcoming the extracellular matrix barrier for oncolytic virotherapy, Gene Ther. 17 (2010) 190–201.
[23] J.S. Lee, M.W. Hur, S.K. Lee, W.I. Choi, Y.G. Kwon, C.O. Yun, A novel sLRP6E1E2 inhibits canonical Wnt signaling, epithelial-to-mesenchymal transition, and induces mitochondria-dependent apoptosis in lung cancer, PLoS One 7 (2012) e36520.
[24] Y. Na, J.W. Choi, D. Kasala, J. Hong, E. Oh, Y. Li, S.J. Jung, S.W. Kim, C.O. Yun, Potent antitumor effect of neurotensin receptor-targeted oncolytic adenovirus co-expressing decorin and Wnt antagonist in an orthotopic pancreatic tumor model, J. Control. Release : Off. J. Control. Release Soc. 220 (2015) 766–782.
[25] E. Kim, J.H. Kim, H.Y. Shin, H. Lee, J.M. Yang, J. Kim, J.H. Sohn, H. Kim, C.O. Yun, Ad-mTERT-delta19, a conditional replication-competent adenovirus driven by the human telomerase promoter, selectively replicates in and elicits cytopathic effect in a cancer cell-specific manner, Hum. Gene Ther. 14 (2003) 1415–1428.

[26] J. Kim, J.H. Kim, K.J. Choi, P.H. Kim, C.O. Yun, E1A- and E1B-Double mutant replicating adenovirus elicits enhanced oncolytic and antitumor effects, Hum. Gene Ther. 18 (2007) 773–786.

[27] C.O. Yun, E. Kim, T. Koo, H. Kim, Y.S. Lee, J.H. Kim, ADP-overexpressing adenovirus elicits enhanced cytopathic effect by induction of apoptosis, Cancer Gene Ther. 12 (2005) 61–71.

[28] N. Zhang, J.-N. Fu, T.-C. Chou, Synergistic combination of microtubule targeting anticancer fludelone with cytoprotective panaxytriol derived from panax ginseng against MX-1 cells in vitro: experimental design and data analysis using the combination index method, Am. J. Canc. Res. 6 (2015) 97–104.

[29] A.M. Crompton, D.H. Kirn, From ONYX-015 to armed vaccinia viruses: the education and evolution of oncolytic virus development, Curr. Cancer Drug Targets 7 (2007) 133–139.

[30] W. Yu, H. Fang, Clinical trials with oncolytic adenovirus in China, Curr. Cancer Drug Targets 7 (2007) 141–148.

[31] M. Liang, Clinical development of oncolytic viruses in China, Curr. Pharmaceut. Biotechnol. 13 (2012) 1852–1857.

[32] M.G. Chai, C. Kim-Fuchs, E. Angst, E.K. Sloan, Bioluminescent orthotopic model of pancreatic cancer progression, J. Vis. Exp. JoVE 76 (2013).

[33] H.L. Weber, M. Gidekel, S. Werbajh, E. Salvatierra, C. Rotondaro, L. Sganga, G.A. Haab, D.T. Curiel, E.G. Cafferata, O.L. Podhajcer, A novel CDC25B promoter-based oncolytic adenovirus inhibited growth of orthotopic human pancreatic tumors in different preclinical models, Clin. Cancer Res. : Off. J. Am. Assoc. Canc. Res. 21 (2015) 1665–1674.

[34] R. Cao, L.P. Wang, Serological diagnosis of liver metastasis in patients with breast cancer, Canc. Biol. Med. 9 (2012) 57–62.

[35] P. Sova, X.W. Ren, S. Ni, K.M. Bernt, J. Mi, N. Kiviat, A. Lieber, A tumor-targeted and conditionally replicating oncolytic adenovirus vector expressing TRAIL for treatment of liver metastases, Mol. Ther. : J. Am. Soc. Gene Ther. 9 (2004) 496–509.

[36] D.M. Gonzalez, D. Medici, Signaling mechanisms of the epithelial-mesenchymal transition, Sci. Signal. 7 (2014) re8.

[37] B. Wu, S.P. Crampton, C.C. Hughes, Wnt signaling induces matrix metalloproteinase expression and regulates T cell transmigration, Immunity 26 (2007) 227–239.

[38] T. Arumugam, V. Ramachandran, K.F. Fournier, H. Wang, L. Marquis, J.L. Abbruzzese, G.E. Gallick, C.D. Logsdon, D.J. McConkey, W. Choi, Epithelial to mesenchymal transition contributes to drug resistance in pancreatic cancer, Cancer Res. 69 (2009) 5820–5828.

[39] J. Kim, J.Y. Cho, J.H. Kim, K.C. Jung, C.O. Yun, Evaluation of E1B gene-attenuated replicating adenoviruses for cancer gene therapy, Cancer Gene Ther. 9 (2002) 725–736.

[40] M. Yamanaka, Y. Tada, K. Kawamura, Q. Li, S. Okamoto, K. Chai, S. Yokoi, M. Liang, T. Fukamachi, H. Kobayashi, N. Yamaguchi, A. Kitamura, H. Shimada, K. Hiroshima, Y. Takiguchi, K. Tatsumi, M. Tagawa, E1B-55 kDa-defective adenoviruses activate p53 in mesothelioma and enhance cytotoxicity of anticancer agents, J. Thorac. Oncol. : Off. Publ. Int. Assoc. Study Lung Canc. 7 (2012) 1850–1857.

[41] G. Wang, G. Li, H. Liu, C. Yang, X. Yang, J. Jin, X. Liu, Q. Qian, W. Qian, E1B 55-kDa deleted, Ad5/F35 fiber chimeric adenovirus, a potential oncolytic agent for B-lymphocytic malignancies, J. Gene Med. 11 (2009) 477–485.

[42] Z. Liang, C.S. Yang, F. Gu, L.S. Zhang, A conditionally replicating adenovirus expressing IL-24 acts synergistically with temozolomide to enhance apoptosis in melanoma cells in vitro, Oncol. Lett. 13 (2017) 4185–4189.

[43] M.A. Thomas, R.S. Broughton, F.D. Goodrum, D.A. Ornelles, E4orf1 limits the oncolytic potential of the E1B-55K deletion mutant adenovirus, J. Virol. 83 (2009) 2406–2416.

[44] B.R. Dix, S.J. O'Carroll, C.J. Myers, S.J. Edwards, A.W. Braithwaite, Efficient induction of cell death by adenoviruses requires binding of E1B55k and p53, Cancer Res. 60 (2000) 2666–2672.

[45] E.J. Kim, J.Y. Yoo, Y.H. Choi, K.J. Ahn, J.D. Lee, C.O. Yun, M. Yun, Imaging of viral thymidine kinase gene expression by replicating oncolytic adenovirus and prediction of therapeutic efficacy, Yonsei Med. J. 49 (2008) 811–818.

[46] A. Rosewell Shaw, M. Suzuki, Recent advances in oncolytic adenovirus therapies for cancer, Curr. Opin. Virol. 21 (2016) 9–15.

[47] E. Eriksson, I. Milenova, J. Wenthe, M. Ståhle, J. Leja-Jarblad, G. Ullenhag, A. Dimberg, R. Moreno, R. Alemany, A. Loskog, Shaping the tumor stroma and sparking immune activation by CD40 and 4-1BB signaling induced by an, Armed Oncolytic Virus 23 (2017) 5846–5857.

[48] T. Ranki, S. Pesonen, A. Hemminki, K. Partanen, K. Kairemo, T. Alanko, J. Lundin, N. Linder, R. Turkki, A. Ristimäki, E. Jäger, J. Karbach, C. Wahle, M. Kankainen, C. Backman, M. von Euler, E. Haavisto, T. Hakonen, R. Heiskanen, T. Joensuu, Phase I Study with ONCOS-102 for the Treatment of Solid Tumors – an Evaluation of Clinical Response and Exploratory Analyses of Immune Markers, (2016).

[49] A. Rodríguez-García, M. Giménez-Alejandre, J.J. Rojas, R. Moreno, M. Bazan-Peregrino, M. Cascalló, R. Alemany, Safety and efficacy of VCN-01, an oncolytic adenovirus combining fiber HSG-binding domain replacement with RGD and hyaluronidase, Expression 21 (2015) 1406–1418.

[50] F.F. Lang, C. Conrad, C. Gomez-Manzano, W.K.A. Yung, R. Sawaya, J.S. Weinberg, S.S. Prabhu, G. Rao, G.N. Fuller, K.D. Aldape, J. Gumin, L.M. Vence, I. Wistuba, J. Rodriguez-Canales, P.A. Villalobos, C.M.F. Dirven, S. Tejada, R.D. Valle, M.M. Alonso, B. Ewald, J.J. Peterkin, F. Tufaro, J. Fueyo, Phase I study of DNX-2401 (Delta-24-RGD) oncolytic adenovirus: replication and immunotherapeutic effects in recurrent malignant glioma, 36 (2018) 1419–1427.

[51] Y.K.S. Man, J.A. Davies, L. Coughlan, C. Pantelidou, A. Blazquez-Moreno, J.F. Marshall, A.L. Parker, G. Hallden, The novel oncolytic adenoviral mutant Ad5-3Delta-A20T retargeted to alphavbeta6 integrins efficiently eliminates pancreatic cancer cells, Mol. Cancer Ther. 17 (2018) 575–587.

[52] E. Eriksson, R. Moreno, I. Milenova, L. Liljenfeldt, L.C. Dieterich, L. Christiansson, H. Karlsson, G. Ullenhag, S.M. Mangsbo, A. Dimberg, R. Alemany, A. Loskog, Activation of myeloid and endothelial cells by CD40L gene therapy supports T-cell expansion and migration into the tumor microenvironment, Gene Ther. 24 (2017) 92–103.

[53] A. Rodriguez-Garcia, M. Gimenez-Alejandre, J.J. Rojas, R. Moreno, M. Bazan-Peregrino, M. Cascallo, R. Alemany, Safety and efficacy of VCN-01, an oncolytic adenovirus combining fiber HSG-binding domain replacement with RGD and hyaluronidase expression, Clin. Cancer Res. : Off. J. Am. Assoc. Canc. Res. 21 (2015) 1406–1418.

[54] X.Z. Wu, F. Ma, X.L. Wang, Serological diagnostic factors for liver metastasis in patients with colorectal cancer, World J. Gastroenterol. 16 (2010) 4084–4088.

[55] M.P. di Magliano, A.V. Biankin, P.W. Heiser, D.A. Cano, P.J. Gutierrez, T. Deramaudt, D. Segara, A.C. Dawson, J.G. Kench, S.M. Henshall, Common activation of canonical Wnt signaling in pancreatic adenocarcinoma, PLoS One 2 (2007) e1155.

[56] L. Wang, D.G. Heidt, C.J. Lee, H. Yang, C.D. Logsdon, L. Zhang, E.R. Fearon, M. Ljungman, D.M. Simeone, Oncogenic function of ATDC in pancreatic cancer through Wnt pathway activation and β-catenin stabilization, Cancer Cell 15 (2009) 207–219.

[57] C.A. Ingraham, G.C. Park, H.P. Makarenkova, K.L. Crossin, Matrix metalloproteinase (MMP)-9 induced by Wnt signaling increases the proliferation and migration of embryonic neural stem cells at low O2 levels, J. Biol. Chem. 286 (2011) 17649–17657.

[58] T. Tanaka, Y. Terai, M. Ohmichi, Association of matrix metalloproteinase-9 and decorin expression with the infiltration of cervical cancer, Oncol. Lett. 17 (2019) 1306–1312.

[59] K. Imai, A. Hiramatsu, D. Fukushima, M.D. Pierschbacher, Y. Okada, Degradation of decorin by matrix metalloproteinases: identification of the cleavage sites, kinetic analyses and transforming growth factor-beta1 release, Biochem. J. 322 (Pt 3) (1997) 809–814.

[60] R.V. Iozzo, D.K. Moscatello, D.J. McQuillan, I. Eichstetter, Decorin is a biological ligand for the epidermal growth factor receptor, J. Biol. Chem. 274 (1999) 4489–4492.

[61] J. Xu, S. Lamouille, R. Derynck, TGF-beta-induced epithelial to mesenchymal transition, Cell Res. 19 (2009) 156–172.

[62] Y. Katsuno, S. Lamouille, R. Derynck, TGF-beta signaling and epithelial-mesenchymal transition in cancer progression, Curr. Opin. Oncol. 25 (2013) 76–84.

[63] J. Harris, H. Bruckner, Adjuvant and neoadjuvant therapies of pancreatic cancer: a review, Int. J. Pancreatol. : Off. J. Int. Assoc. Pancreatol. 29 (2001) 1–7.

[64] G. Szakacs, J.K. Paterson, J.A. Ludwig, C. Booth-Genthe, M.M. Gottesman, Targeting multidrug resistance in cancer, Nat. Rev. Drug Discov. 5 (2006) 219–234.

[65] A.I. Minchinton, I.F. Tannock, Drug penetration in solid tumours, Nature reviews, Cancer 6 (2006) 583–592.

[66] Z. Wang, Y. Li, A. Ahmad, S. Banerjee, A.S. Azmi, D. Kong, F.H. Sarkar, Pancreatic cancer: understanding and overcoming chemoresistance, Nature reviews, Gastroenterol. Hepatol. 8 (2011) 27–33.

[67] A. Voulgari, A. Pintzas, Epithelial-mesenchymal transition in cancer metastasis: mechanisms, markers and strategies to overcome drug resistance in the clinic, Biochim. Biophys. Acta 1796 (2009) 75–90.

[68] R. Shao, D. Karunagaran, B.P. Zhou, K. Li, S.S. Lo, J. Deng, P. Chiao, M.C. Hung, Inhibition of nuclear factor-kappaB activity is involved in E1A-mediated sensitization of radiation-induced apoptosis, J. Biol. Chem. 272 (1997) 32739–32742.

[69] S.W. Lowe, H.E. Ruley, T. Jacks, D.E. Housman, p53-dependent apoptosis modulates the cytotoxicity of anticancer agents, Cell 74 (1993) 957–967.

[70] Y. Hu, H. Sun, R.T. Owens, J. Wu, Y.Q. Chen, I.M. Berquin, D. Perry, J.T. O'Flaherty, I.J. Edwards, Decorin suppresses prostate tumor growth through inhibition of epidermal growth factor and androgen receptor pathways, Neoplasia 11 (2009) 1042–1053.

[71] Y. Fujita, M. Kitagawa, S. Nakamura, K. Azuma, G. Ishii, M. Higashi, H. Kishi, T. Hiwasa, K. Koda, N. Nakajima, K. Harigaya, CD44 signaling through focal adhesion kinase and its anti-apoptotic effect, FEBS Lett. 528 (2002) 101–108.

[72] C.S. Mitsiades, N. Mitsiades, M. Koutsilieris, The Akt pathway: molecular targets for anti-cancer drug development, Curr. Cancer Drug Targets 4 (2004) 235–256.

[73] C.H. Heldin, K. Rubin, K. Pietras, A. Ostman, High interstitial fluid pressure - an obstacle in cancer therapy, Nat. Rev. Canc. 4 (2004) 806–813.

[74] C.J. Whatcott, R.G. Posner, D.D. Von Hoff, H. Han, Desmoplasia and Chemoresistance in Pancreatic Cancer, (2012).

[75] S. Dangi-Garimella, S.B. Krantz, M.R. Barron, M.A. Shields, M.J. Heiferman, P.J. Grippo, D.J. Bentrem, H.G. Munshi, Three-dimensional collagen I promotes gemcitabine resistance in pancreatic cancer through MT1-MMP-mediated expression of HMGA2, Cancer Res. 71 (2011) 1019–1028.

[76] P.S. Hodkinson, A.C. Mackinnon, T. Sethi, Extracellular matrix regulation of drug resistance in small-cell lung cancer, Int. J. Radiat. Biol. 83 (2007) 733–741.